JPRS 78585

23 July 1981

China Report

SCIENCE AND TECHNOLOGY

No. 112

FBIS FOREIGN BROADCAST INFORMATION SERVICE

NOTE

JPRS publications contain information primarily from foreign newspapers, periodicals and books, but also from news agency transmissions and broadcasts. Materials from foreign-language sources are translated; those from English-language sources are transcribed or reprinted, with the original phrasing and other characteristics retained.

Headlines, editorial reports, and material enclosed in brackets [] are supplied by JPRS. Processing indicators such as [Text] or [Excerpt] in the first line of each item, or following the last line of a brief, indicate how the original information was processed. Where no processing indicator is given, the information was summarized or extracted.

Unfamiliar names rendered phonetically or transliterated are enclosed in parentheses. Words or names preceded by a question mark and enclosed in parentheses were not clear in the original but have been supplied as appropriate in context. Other unattributed parenthetical notes within the body of an item originate with the source. Times within items are as given by source.

The contents of this publication in no way represent the policies, views or attitudes of the U.S. Government.

PROCUREMENT OF PUBLICATIONS

JPRS publications may be ordered from the National Technical Information Service, Springfield, Virginia 22161. In ordering, it is recommended that the JPRS number, title, date and author, if applicable, of publication be cited.

Current JPRS publications are announced in Government Reports Announcements issued semi-monthly by the National Technical Information Service, and are listed in the Monthly Catalog of U.S. Government Publications issued by the Superintendent of Documents, U.S. Government Printing Office, Washington, D.C. 20402.

Indexes to this report (by keyword, author, personal names, title and series) are available from Bell & Howell, Old Mansfield Road, Wooster, Ohio 44691.

Correspondence pertaining to matters other than procurement may be addressed to Joint Publications Research Service, 1000 North Glebe Road, Arlington, Virginia 22201.

JPRS 78585

23 July 1981

CHINA REPORT

SCIENCE AND TECHNOLOGY

No. 112

CONTENTS

PEOPLE'S REPUBLIC OF CHINA

PHYSICAL SCIENCES

Prospects for Developing Nuclear Power Stations Outlined
(Jia Hongbin; DIAN SHIJIE, Mar 81) 1

APPLIED SCIENCES

Breakthrough in Chinese Language Computer Described
(Zhou Wenbin; GUANGMING RIBAO, 10 Jun 81) 5

Digital Processing of Remote Sensing Information Discussed
(Xu Jianhua; DIANZI JISHU, 20 Dec 80) 6

New Cosmic Dust Discovered in Atmosphere, Ancient Strata
(Xiao Zhong; GUANGMING RIBAO, 16 Jun 81) 16

Electroflotation of Lead-Zinc Ore Described
(Liu Jingwen; YOUSE JINSHU, No 2, 1981) 18

National Symposium on Tungsten Research Held
(YOUSE JINSHU, No 2, 1981) 19

First Symposium of Technological Mineralogy Held
(YOUSE JINSHU, No 2, 1981) 21

Heat Treatment for Processed Beryllium Bronze Described
(Zhou Shanyou; JINSHU RECHULI, No 4, 1981) 25

PUBLICATIONS

Table of Contents of 'JISUANJI XUEBAO' Nos 1-3, 1981 41

[III - CC - 84]

Table of Contents of 'FUDAN XUEBAO (ZIRAN KEXUE BAN)' No 1, 1981... 45

Table of Contents of 'XI'AN JIAOTONG DAXUE' No 2, 1981 47

Table of Contents of 'WULI' No 3, 1981 49

ABSTRACTS

METALLURGY

JINSHU XUEBAO [ACTA METALLURGICA SINICA] No 2, Apr 81 52

SOLAR ENERGY

TAIYANGNENG XUEBAO [ACTA ENERGIAE SOLARIS SINICA] No 2, Apr 81..... 64

PHYSICAL SCIENCES

PROSPECTS FOR DEVELOPING NUCLEAR POWER STATIONS OUTLINED

Shanghai DIAN SHIJIE [WORLD OF ELECTRICITY] in Chinese No 3, Mar 81 pp 1-2

Article by Jia Hongbin [6328 7703 2430] of the Huadong Electrical Power Design Institute: "Prospect of the Development of Nuclear Power Stations in Our Nation in the 1980's; Utilization and Conservation of Energy"]

[Text] The energy resource utilized to build power stations in our nation has always been mainly coal and hydraulic power (in recent years, some power stations that use fuel have emerged but looking at the trend, they are not the future direction). Coal is mostly produced in the northwest and the north. Hydraulic power is mostly located in the southwest and the southern provinces. But the coastal regions where industry is developed lack energy resources, causing "northern coal to be shipped to the south". A thermogenerator of 300,000 kilowatts of power each year consumes about 27 million tons of coal. But a nuclear generator of 900,000 kilowatts of power requires changing part of the fuel only once a year and each change requires only 24 tons of fuel. In addition, coal and petroleum are both important chemical and industrial raw materials affecting the nation and the people's livelihood, and using them as fuel seems to be a pity. Therefore, developing the nuclear power station is a direction.

At present, the nuclear stations built by most nations only utilize the first step of atomic energy, only utilizing the thermal energy produced by fission of uranium 235 (U^{235}) to generate electricity. This method has a very low percentage of utilization of nuclear energy. One ton of uranium is only equivalent to 300,000 tons of coal. Therefore, the second step of utilization of nuclear energy must be developed, that is, to utilize uranium 235 to produce thermal energy and to utilize its radiation energy to change thorium into a new energy source, plutonium 239, which does not exist naturally. After such a conversion, the energy in thorium resources can be released, thus making 1 ton of uranium become the equivalent of 1 million tons of coal. Now, some nations have already reached the second step. Our nation has a relatively rich thorium mineral resource. Developing this type of "thorium breeder" reactor will push our nation's utilization of nuclear energy towards a new stage. The third step in the utilization of nuclear energy is controlled thermonuclear reaction. When fusion is used to produce heat to generate electricity, then the energy situation will undergo a fundamental change.

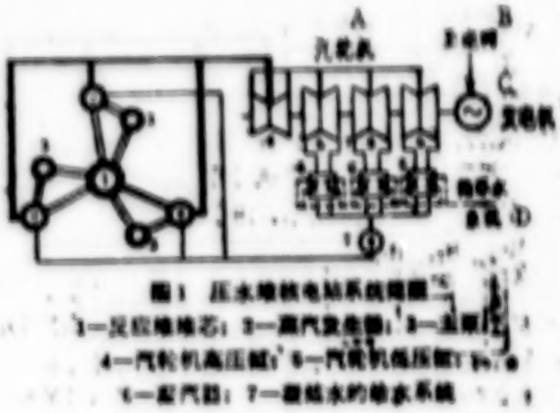

Figure 1 Simplified diagram of the nuclear power station system with a pressured water reactor

1. Reactor core
2. Steam generator
3. Main pump
4. High pressure cylinder of the turbogenerator
5. Low pressure cylinder of the turbogenerator
6. Steam condenser
7. Water supply system of condenser water

A. Turbogenerator
B. To power network
C. Power generator
D. Water circulation system

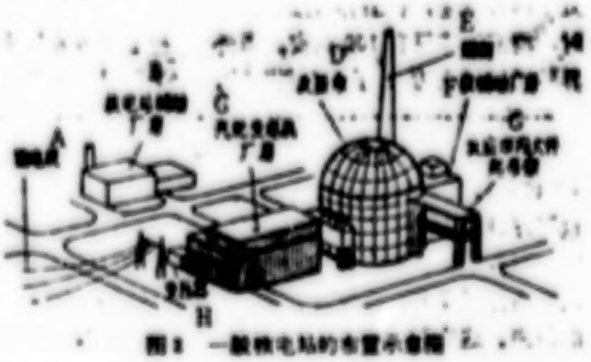

Figure 2 Illustrative layout of an ordinary nuclear power station

A. Power Supply line
B. Auxiliary room of the nuclear power station
C. Turbogenerator housing
D. Reactor
E. Smoke stack
F. Nuclear auxiliary shop
G. Hanger for large objects in reactor
H. Transformer

Prospect of Our Nation's Nuclear Power Stations

While our nation builds her own nuclear power stations, it is possible to introduce some equipment from abroad. For example, the pressurized water reactor is a type of light water reactor, it is also the type that is most commonly used in the world at present. But it still belongs to the first step of utilization of nuclear energy. A nuclear power station with a one million kilowatt class light water reactor generates power at a cost which is 1/3 the cost of generating electric power by a thermal power station of the same capacity but the investment is only 1.5 times higher than that of a thermal power station. At the same time, this type of reactor has a longer operating experience, the accident rate and the time of fuel change have dropped and shortened over the years. Its greatest advantage is that it can accumulate for us the experience of producing plutonium 239 and extracting plutonium 239 and establish the foundation for developing the breeder reactor.

The reactor of this type of nuclear power station has three closed cooling loops as shown in Figure 1, abbreviated the triple loop. In each loop there is a steam generator and a main pump. Each loop is filled with water containing boron. Driven by the main pump, the water containing boron circulates in the closed loops through the reactor core, the steam generator and the main pump. The water containing boron carries the heat of the reactor core to the steam generator. Here, the heat is transfered to the condenser water which evaporates and produces steam to drive the turbogenerator for power generation. The reactor core contains low enriched uranium as fuel totaling 72.5 tons. This amount can generate 2,775,000 kilowatts of thermal power. Each year, only 1/3 of the fuel needs to be changed to new fuel, and only one change a year is needed. The three steam generators provide 5446.8 tons of steam per hour to the turbogenerator. The pressure of the steam is 57.7 bar (1 bar = 0.986923 standard atmospheric pressure), the temperature is 271°C, humidity is 0.25 percent. The turbogenerator has one high pressure cylinder, three low pressure cylinders, and it is of the dual flow impulse type. It drives the power generator which can produce 966,000 kilowatts of electricity. At the same time, the turbogenerator also needs about 150,000 tons of circulating water per hour to cool the steam condenser. Because of the large amount of water used, it is more reasonable to locate it in the coastal region. Figure 2 illustrates the layout of an ordinary nuclear power station.

The larger the power of the nuclear power station, the lower the corresponding investment and cost. At present, the world still tends to build single unit generators with power above the 1 million kilowatt class. This type of a large capacity nuclear power station has brought some new topics to our nation's electrical power industry, equipment manufacturing, electronics industry and technical management.

1. Because nuclear power stations have radioactivity, a lot of equipment is frequently used to the end of its life (40 years) and is not allowed to be repaired or replaced. In some areas, even people are not allowed to enter. Therefore, the equipment requires a high degree of reliability and durability. Operating personnel can only judge the operating state of the nuclear power station by the parameters reflected by the various display systems and the operating state computed by the computational system. Then corresponding measures are carried out. These are all requirements that have not occurred in thermal power stations.

2. Nuclear energy is a newly opened energy resource in our nation. Related laws, regulations and standards must be quickly established. Although the International Atomic Energy Commission has established some standards, they are incomplete and they do not necessarily suit our nation's situation. Especially regarding the question of safety standards, laws taking into consideration our nation's situation and suitable for our nation should be established.

At present, the selection of sites for nuclear power stations internationally tends to avoid regions of dense population. Our nation's coastal electric power industry needs energy resources but the population is also very dense, if the site is selected according to foreign standards (meaning the standard of population density), this will cause great difficulty. Therefore, besides considering meeting the demands of environmental protection, the population density standard near our nation's nuclear power station should be established according to the allowable dosage of radioactivity resulting from normal accidents at nuclear power stations.

3. In 1979, after the "Three Mile Island incident" in the United States, the development of nuclear power in the United States encountered a great setback. People opposing nuclear power stations are mainly worried about the safety of nuclear power stations, the handling of radioactive "three wastes" during ordinary times, how to handle nuclear power stations that will have been completely scrapped at the end of their useful life (40 years). Concerning these questions, our nation should also take them into full consideration at the beginning period of developing nuclear power generation.

In addition, fuel policy, transportation of radioactive materials, prevention of earthquakes for nuclear power stations and its geological requirements should all be studied and determined at the same time. But it can be foreseen that the 1980's will be a new period of development of nuclear power stations in our nation.

9296
CSO: 8111/1266

BREAKTHROUGH IN CHINESE LANGUAGE COMPUTER DESCRIBED

Beijing GUANGMING RIBAO in Chinese 10 Jun 81 p 1

[Article by Zhou Wenbin [0719 2429 2430]: "Invention for Chinese Language Computer Registered for International Patent"]

[Text] There have been a series of breakthroughs in China's research on a Chinese language computer in recent years. In early May, Beijing Normal University instructor Li Jinkai [2621 6855 6963] was invited to Hong Kong to report on his invention on the "Chinese character stroke compiler code" and was praised by Hong Kong experts and professors. They believe that Li's coding method is "so far the most ideal proposal for a Chinese language computer." This invention has been registered for international patent in England.

Li Jinkai has been working on a coding method for Chinese character strokes in his spare time for almost 20 years. As early as 1961, Li collaborated with the famous scholar Ding Xilin [0002 6007 2651], now deceased, and part-time school instructor Li Yimin [2621 3015 3046] and proposed a "stroke searching method for Chinese characters." This search method was later evaluated and recommended by the Ministry of Culture and the Ministry of Education, and in October 1965 the Culture and Education Office of the State Council directed the relevant departments to test-use the searching method. During the 10-year disaster of the Culture Revolution, although the test-use promotion work was forced to halt, research on the coding method for Chinese characters for input into a Chinese language computer continued. In 1978, Li Jinkai finally completed his important invention with the assistance of Li Yimin.

The most difficult task for a Chinese language computer is the input of Chinese character signals. The big keyboard popular in Japan is difficult to learn, the input speed is slow, and it requires very expensive special equipment. The unique features of the "Chinese character stroke compiler coding method" are that it is easy to learn and can be entered into the computer at a high speed. A junior-high school student can grasp this coding method in only one hour, and with practice the input speed can reach 4,600 characters per hour or higher. Since this coding method is totally unrelated to the pronunciation of the Chinese characters, foreigners not knowing Chinese can also use it. Moreover, the input process does not require the addition of any special equipment; it can be done with a regular computer keyboard.

Looking up words in dictionaries compiled with this character stroke compiler code is found to be at least twice as fast as in old methods. A combination of the searching method for a dictionary and the character stroke compiler code for a Chinese language computer will be highly significant in the promotion of Chinese language computers.

9698
CSO: 4008/387

APPLIED SCIENCES

DIGITAL PROCESSING OF REMOTE SENSING INFORMATION DISCUSSED

Shanghai DIANZI JISHU [ELECTRONIC TECHNOLOGY] in Chinese No 12, 20 Dec 80 pp 1-4

[Article by Xu Jianhua [1776 1696 5478]: "Digital Processing of Remote Sensing Information, Part 1"]

[Text] The macroscopic, large-area raw data obtained from aerospace platforms (satellites, spacecraft, aircraft) by means of sensors (multispectrum photography, multispectrum scanning, active and passive microwave systems) can be processed by digital computers, producing useful information about the object of study; this is called "digital processing of remote sensing information."

The raw data can be stored on magnetic tape, then relayed to a computer for processing after returning to earth; or it can be sent from aloft by radio to the computer; or it can be subjected to necessary preprocessing on board the platform (see Figure 1):

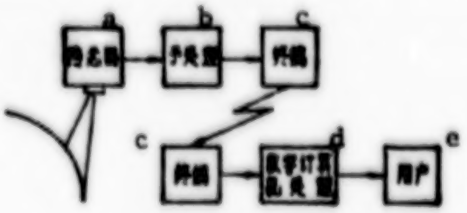

Figure 1. Remote Sensing Information Processing System

Key:
- a. Sensor
- b. Preprocessing
- c. Terminal
- d. Processing by digital computer
- e. User

Systems which transmit information by radio from the aerospace platform to the computer can be either real-time or nonreal-time systems. Real-time processing makes very high demands on processing methods, software and hardware.

We can use digital computers and hybrid optical processing systems to solve the problem of high-speed real-time processing hardware.

Macroscopically, the use of multispectrum scanners and microwave remote sensors and the use of aerospace platforms to carry them aloft expand man's visual perception system from the visible region into the ultraviolet, infrared and microwave regions and widen his field of vision to include the globe and space.

Digital processing of remote sensing information can compress the data rate, improve image quality, filter out noise, eliminate blurring and correct distortion. The use of precise numerical concepts to assess and describe the markings and forms of the area being observed makes possible recognition and classification of terrain features. Use of a digital computer for description and classification of images is also a topic in the field of artificial intelligence. Increasing machine efficiency and simulating the mechanisms of the human brain ultimately can effectively help or supplant interpretation experts in many fields in recognizing remote sensing images. This is an extremely attractive objective.

1. Digital Processing of Remote Sensing Images

A. Digitization and Compression of the Image

If we sample an image, we obtain a discrete image, i.e. an M x N matrix $[f_{i,j}]$, where $i = 0, 1, \ldots, M$ and $j = 0, 1, \ldots, N$, and $f_{i,j}$ is the grayness of the image element in the i-th line and j-th column. The quantization order is $2^8 - 2^{10}$ (8 to 10 bits) in high-resolution imaging. The United States LANDSAT 1-3 satellites all use 6 bits, while LANDSAT 4 uses 8 bits. The sampled and quantized image requires a very large number of storage bits. For the 9-inch LANDSAT 1 images, with $N = 2340$ and $M = 3240$, an image requires about 7.6×10^6 image elements, and if these are quantized with 8 bits, a total of 6×10^7 bits is required for storing and transmitting the image; with images taken in 4 different wavelengths, the requirement is for 240 million bits. In order to save memory space and increase transmission efficiency, the image $[f_{i,j}]$ can be compressed.

The main technique of image compression is transformation compression. A given image is subjected to an invertable transformation and the transformed image approximated, after which the inversion is effected to construct a new image. For example, the Fourier transform of $[f_{i,j}]$ produces $[F_{u,v}]$, but because man's visual perception system is of a bandpass character, $F_{u,v}$ can be ignored for rather large u,v, and by standardizing $F_{u,v}$ an approximation $[F_{u,v}]$ can be obtained and transmitted to another terminal or stored is external memory, thus greatly decreasing the information rate, and when the image is to be recovered at the receiving terminal or fetched from storage, an approximation $[f_{i,j}]$ of the original image can be obtained by inversion of $[F_{u,v}]$.

Other methods of transformation compression include slant transform and cosine transform compression.

Another method of image compression is forecasting compression.

B. Normalizing Image Grayness and Tone

Because the illumination of the film is uneven, the amount of light energy falling on the center of a film is greater than that falling at the edge. Changes in exposure, the sun, cloud, atmospheric turbidity and the observing angle can sometimes make part or all of the object observed become brighter or darker; in microwave remote sensing changes in the humidity can produce this phenomenon, as can cloud cover in multispectrum scanning.

If we are interested in distinguishing different types of crops on the ground surface and the information on crop types involves only differences between spectral regions and not intensity, we can calculate the normalized intensity for an image element (m, n): $\bar{x}_i(m, n) = x_i(m, n) / \sum_{i=1}^{n} a_i x_i(m, n);$

where $x_i(m, n)$ ($i = 1, 2, \ldots, n$) is the intensity in the i-th section of the spectrum at point (m, n), and $\{a_i\}$ is a weighting factor. In processing of this type, intensity differences at the various points of the original image are suppressed, so as to bring out differences between channels.

Normalization of changes resulting from differences in atmospheric smog or turbidity or the observing angle takes account of the fact that when the frequency range is small enough, backscattering can be ignored, and we obtain $R_{\tau 1}/R_{\tau 2} = \rho_1/\rho_2$ (where R_τ is the radiant intensity detected by the sensor and ρ is the standard reflectivity). Accordingly, by using the ratio of the radiation intensity obtained in two neighboring spectral regions it is possible to suppress changes resulting from differences in atmospheric smog or turbidity and the observing angle, thus bringing out the relative change ρ_1/ρ_2 in the reflectivity characteristics of the object in which we are interested. Thus an N-spectral region (N-channel) multispectrum scanner (N = 4 for the LANDSAT 1) obtains an n-dimensional vector $(x_1, x_2, \ldots, x_N)$ for the radiative intensity, which can be normalized into an (N-1)-dimensional vector $(x_1/x_2, x_2/x_3, \ldots, x_{N-1}/x_N)$, where x_i is the radiant intensity (energy) in the i-th channel ($i = 1, 2, \ldots, N$). If we allow for the backscatter effect and if within a sufficiently small spectral region the light source radiative intensity, the atmospheric transmissivity and the backscatter are all constant, we can normalize as follows:

$$\left(\frac{x_1 - x_2}{x_2 - x_3}, \frac{x_2 - x_3}{x_3 - x_4}, \ldots, \frac{x_{N-2} - x_{N-1}}{x_{N-1} - x_N}\right)$$

C. Image Matching and Superposition and Geometrical Distortion Correction

Images taken at different times in a given spectral region or in different spectral regions at the same time must be matched and superposed and stored in internal or external memory in such a way that all corresponding points match. Shifting or rotating two images to achieve maximum correlation is called matching. Matching up of images of different geometric shape (distorted) is called superposition. Two methods that can be used to correct distorted images are described below.

(1) Positioning by ground-based control points. Ground-based control points are characteristics or ground markers which are visible in the image and whose geographic coordinates can be determined. By using these control points it is possible to set up a relationship between the geometric shape of the image and the required map projection; manual and automatic methods can be used to determine the control points' image coordinates.

(2) Establishing overall illumination coefficient. Suppose the coordinates of the geometric distortion are (x, y), and the original image coordinates are (u, v). Let $T_{\vec{\alpha}}$ be the coordinate transformation from (x, y) to (u, v). Distortion correction involves setting up the relationship:

$$f(u, v) = f[T_{\alpha}(x, y)].$$

In we take $T_{\vec{a}}$ as an affine transformation, then (using [x] to express the integer closest t x),

$$\begin{cases} u=[Ax+By+C] \\ v=[Dx+Ey+F] \end{cases} \qquad f(u, v)=f([Ax+By+C], [Dx+Ey+F])$$

here $\vec{a}$ = (A, B, C, D, E, F). If A = E = 1, B = D = 0, it is purely translational; if C = F = 0, $A^2 + B^2 = D^2 + E^2 = 1$, it is purely rotational; if A/B = D/E, C = F = 0 it is a change of scale.

It is also possible to make $T_{\vec{a}}$ a projection transformation, a K = th order polynomial transformation and the like.

The above parameters can be determined using ground control points. For example, for the affine transformation, the coefficients A, B, C, D, E, and F can be solved by substituting the coordinates of three control points not on the same line (scattered over the image to be rectified) and the actual image coordinates into the above transformation formula to obtain three groups of formulas. Changes in the horizontal-vertical ratio and crookedness can both be corrected by this method.

Simple geometric distortions (such as translation) can be corrected by means of correlation measurements and distance measurements; for examples, see references [1] and [2] [not reproduced].

D. Image Intensification and Filtering

In the process from image photographing, scanning and transmission to storage and display, many factors result in a rather considerable decline in image quality compared with the original object. The image obtained is generally blurred and contains noise interference. It can be improved by computer processing. Correction of the brightness scale (increasing contrast), elimination of blurring (bringing out edges), elimination of noise (smoothing) and use of digital filtering, Karman filtering and self-adaptive filtering are methods of intensifying the image.

1. Adjustment of the Brightness Scale: Because objects at different distances from the optical axis of the system and different points scanned by the scanning tube are recorded with different sensitivities, the image grayness and the brightness of the terrain do not match up: images with the same brightness do not match up with terrain areas with the same brightness. The method of eliminating this effect is as follows: suppose that f(x, y) is the ideal grayness, and the nonuniform image obtained is Q (x, y) = e (x, y) · f (x, y), where e (x, y) is a function of the instrument characteristics. For a terrain feature D with a known uniform brightness, f (x, y) = C (a constant), (x, y) ∈ D. Let Q_C (x, y) be the image obtained from that terrain feature: then e (x, y) equals e (x, y) = Q_C (x, y)/C. Finally a grayness correction can be made for all other parts of the image with (x, y) not belonging to D:

$$f(x, y) = C \cdot Q(x, y)/Q_C(x, y)$$

The method of increasing contrast is as follows: if the image quantification order is K, the range of variation of grayness is $[Z_1, Z_k]$, and the image grayness range obtained is $[a, b] \subset [Z_1, Z_k]$ (e.g. with insufficient exposure), we can make the following transformation:

$$Z' = \frac{Z_k - Z_1}{b-a} Z + \frac{Z_1 b - Z_k a}{b-a}, \quad Z \in [a, b]$$

The contrast of an image reconstructed using the Z' obtained will be greater than that of the original. We can also excise a certain section of [a, b] and compress the other parts.

We can also use a histogram adjustment to improve image quality.

We make a grayness distribution histogram (Figure 2a) for an image, in which p_i is the number of image elements with grayness Z_i. The histogram correction involves using this brightness of order K to make a new histogram (Figure 2b), such that $\sum_{i=1}^{k} q_i = \sum_{i=1}^{k} p_i$. If the histogram after correction is flatter, the new image constructed using it will have higher contrast and will be intensified.

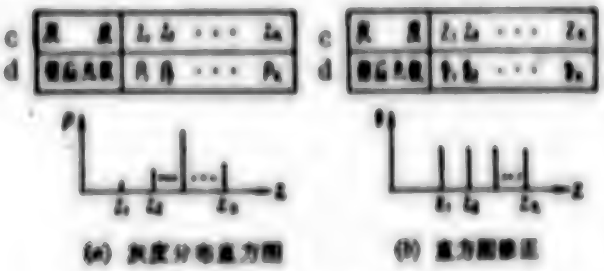

Figure 2

Key: a. Grayness distribution histogram
b. Histogram correction
c. Grayness
d. Relative number of points

2. A simple method of eliminating blurring (bringing out edges): The reason for image blurring is always an effect resulting from an averaging or integrating operation. Accordingly, a simple method for removing blurring is to perform a differentiating or subtracting operation on the image. Because the blurred object (e.g. a boundary or a diameter) can be in any direction, the integral operation for the desired structure is isotropic. For example, we take the Laplacian of the image: for every (i, j) we take

$$\begin{aligned}\nabla^2 f(i,j) &\triangleq \Delta_x^2 f(i,j) + \Delta_y^2 f(i,j) \\ &= [f(i+1,j) + f(i-1,j) \\ &\quad + f(i,j+1) + f(i,j-1)] - 4f(i,j)\end{aligned}$$

Here, Δ_x and Δ_y express a first-order difference, and Δ_x^2 and Δ_y^2 express second-order differences; this operation brings out the part of the image which has high-frequency spatial changes.

If we denote the blurred image was $Q(i, j)$ and multiply $\nabla^2 Q$ by a positive factor K, then reverse the sign and add it to the blurred image, i.e. $Q(i, j) - K \nabla^2 G(i, j)$, we have an excellent approximation of the original image $f(i, j)$, and we bring out the boundaries. If we set $K = 1$, then

$$\begin{aligned} Q(i, j) - \nabla^2 Q(i, j) = Q(i, j) \\ + 5\Big\{ Q(i, j) - \frac{1}{5}[Q(i+1, j) \\ + Q(i, j+1) + Q(i, j) \\ + Q(i-1, j) + Q(i, j-1)]\Big\}; \end{aligned}$$

The second term on the right of this equation is 5 times the result of subtracting from the initial image an image from which the high-frequency component has been filtered out and the low frequencies left intact, i.e. $5(Q-\bar{Q})$, thus preserving and strengthening the completed high frequency component. Adding this term to Q, both preserves all the original spatial frequencies and strengthens the high frequency (boundary) components. A blurred sensor image of a lunar volcanic crater resulting from atmospheric turbulence has been subjected to this type of filtering with excellent results.

3. A Simple Method of Eliminating Noise (Smoothing): The main difficulty in filtering images with noise interference is preventing blurring of the image (i.e. of the boundaries). In frequency terms, we eliminate the high-frequency component. Spatially, we perform some averaging of the image. In order to prevent blurring of boundaries with crisp contours, we may first measure the boundaries and straight lines, and when filtering noise we operate only in the areas that do not include these boundaries and straight lines.

4. Two-Dimensional Digital Filtering: An image which has undergone low-pass filtering maintains much image information, but has lost crisp contours and detail; an image which has undergone high-pass filtering maintains contours and detail crispness and contrast, but it has lost information from the constant-grayness areas. By means of combined low-pass, bandpass and high-pass two-dimensional filtering we can make a false-color composite image in terms of spatial frequency; a simplified diagram is shown in Figure 3.

For multiplicatively-combined image graynesses $f(x, y) = i(x, y) \cdot r(x, y)$ we can use same-state filtering, a simplified diagram of which is shown in Figure 4.

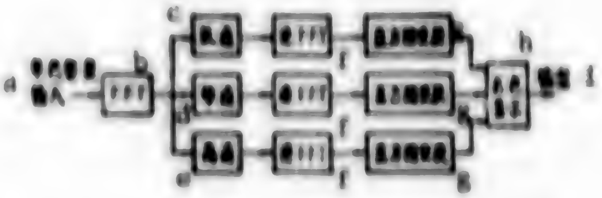

Figure 3. Spatial-Frequency False-Color Composite Imaging

Key:

a. Single-color image input	e. High-pass
b. Fast Fourier transformation	f. Inverse fast Fourier transformation
c. Low-pass	g. Histogram transformation
d. Bandpass	h. Color display
	i. Output

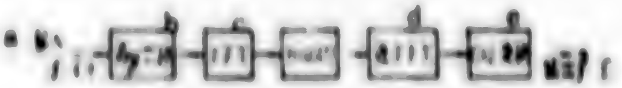

Figure 4. Two-Dimensional Same-State Filtering To Eliminate Product-Type Noise

Key:

a. Input	d. Inverse fast Fourier transformation
b. Long transformation	e. Exponential transformation
c. Fast Fourier transformation	f. Output

Here, H(u, v) is the filter transfer function. If i(x, y) gives the incident illumination and r(x, y) the reflectivity, by performing an exponential transformation we obtain

$$\log f(x, y) = \log i(x, y) + \log r(x, y);$$

The incident illumination i(x, y) generally lags behind the changes in the reflectance r(x, y). If we use a high-pass filter transfer function for H(u, v), we can filter i(x, y) and obtain the required information on the image reflectivity r(x, y). If we use a same-state filter we can strengthen the reflected-light [niguang 6627 0342] image. If we use the Wiener [phonetic] filter transfer function in processing LANDSAT images obtained in cloud cover, we can eliminate the cloud cover.

5. Karman Filtering and Self-Adaptive Filtering: We can make use of the digital computer's suitability for recursive calculations and real-time processing by using the Karman recursive method to strengthen blurred images with noise interference. In order to prevent blurring of sharp images and detail, we can use self-adapting filtering to detect various line and structural components of the images and can adjust the filter parameters in real time so that the filtering effects are enhanced.

E. Image Recovery

In high-altitude reconnaissance and resource sensing images, atmospheric turbulence, optical system deviation and relative movement of the camera and object during exposure produce blurring. Let the ideal image grayness be f(x, y) and the blurred image be Q(x, y). The type of blurring described can be described in the following formula:

$$Q(x, y) = \iint h(x, y; x', y') f(x', y') dx'dy' + v(x, y);$$

Here h(x, y; x', y') is called the point diffusion coefficient, which is known and can be estimated; v(x, y) is random noise. The above equation expresses the fact that the image blurring is caused by two factors: first, that the grayness Q(x, y) of a certain point (x, y) on the blurred image is contributed to by all points in the ideal image f(x', y') (with weighting factor h); second, that there is an effect from random interference. How can we estimate the ideal image f(x, y) from the blurred image Q(x, y)? This is a problem of image grayness. Clearly, the two central problems affecting recovery are: how to determine the point diffusion coefficient h(x, y' x', y'), and, once h(x, y; x', y') is specified, finding effective methods for obtaining from Q(x, y) an estimate f(x, y) for the function $\tilde{f}(x, y)$.

Some special point diffusion coefficients can be inferred from physical phenomena themselves, for example blurring resulting from relative movement of the camera and the objective during exposure. Some coefficients can be estimated from the image itself on the basis of some clear points, lines and boundaries.

1. Inverse Filtering For a linear spatially constant h(x, y; x', y') ≡ h(x-x'; y-y'); if v(x, y) ≡ 0, then if at the two sides we obtain the Fourier transform and denote the changes in Q, h and f as G, H and F respectively, then

$$G(u, v) = H(u, v) F(u, v)$$

or

$$F(u, v) = G(u, v)/H(u, v)$$

If we recover F(u, v) from G(u, v) and obtain an estimate f(x, y) for $\tilde{f}(x, y)$, the transfer function is 1/H(u, v): this is inverse filtering. If after we obtain F(u, v) we take the inverse Fourier transform, we obtain $\tilde{f}(x, y)$.

To eliminate H(u, v) = 0 and to determine G(u, v) when V(u, v) exists, we use the following inverse filtering transfer function:

$$M(u, v) = \begin{cases} 1/H(u, v), & \text{where} \quad u^2+v^2<w_0^2; \\ 1, & \text{where} \quad u^2+v^2>w_0^2, \end{cases}$$

where w_0 is a constant suitably chosen so that H(u, v) does not have a zero within $u^2 + v^2 \leqslant w_0^2$. A diagram is shown in Figure 5.

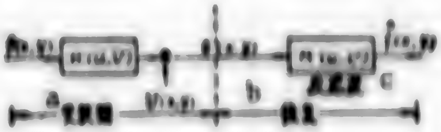

Figure 5. Inverse Filtering

Key: a. Blurring b. Recovery c. Inverse filter

2. Wiener Filtering: Because the estimate f(x, y) of $\overline{f}(x, y)$ obtained by inverse filtering involves a compromise, the filtering result has a certain amount of indeterminacy. Noting that

$$Q(x, y)=\iint h(x-x', y-y')f(x', y')dx'dy' + v(x, y),$$

so-called Wiener filtering is performed as follows: if we let {f} be a homogeneous random field, and if the power spectra S_{ff} and S_{vv} of f and v are known, on the basis of Q we seek an estimate f for $\overline{f}$ such that

$$E[f-\overline{f}]^2=\min;$$

i.e. the extent to which the estimate $\overline{f}$ and found from Q approximates the function f which it estimates is such that it minimizes the mean square difference between f and $\overline{f}$. Accordingly the Weiner filter is also called the mean square filter. It can be proved that if Q is the input and $\overline{f}$ is the output, the Weiner filter transfer function is

$$M(u, v)=\frac{1}{H(u, v)}\cdot\frac{|H(u, v)|^2}{|H(u, v)|^2+[S_{vv}(u, v)/S_{ff}(u, v)]}$$

If S_{vv} = 0 and M(u, v) = 1/H(u, v), the Weiner filter is converted into an ideal inverse filter.

If v(x, y) is white noise, then $S_{vv}(u, v) \equiv a$ (constant), and this constant a can be estimated by the following formula (R_{vv} is the self-correlation coefficient of v):

$$a=S_{vv}(0, 0)=\iint_{-\infty}^{\infty} R_{vv}(x, y)dxdy;$$

If the homogeneous random field is also ergodic, then R_{vv} can be calculated by calculating the estimated spatial self-correlation coefficient from an image that only contains noise (setting f ≡ 0). If S_{ff} and S_{vv} are both unknown, we can approximate as follows:

$$M(u, v)=\frac{1}{H(u, v)}\,\frac{|H(u, v)|^2}{|H(u, v)|^2+\Gamma}$$

Here Γ is a suitably chosen constant which expresses the ratio between noise and the signal power spectrum. If we use the Weiner filter to recover a LANDSAT 1 image obtained with thin cloud cover, we can eliminate the cloud cover effect. The results from use of Wiener filtering to recover an image blurred by motion are better than those obtained with inverse filtering.

There is another method of image recovery in the frequency domain, namely "constrained inverse faltung." It requires only that we know the noise variance σ_v^2; under certain constraints the estimate $\hat{f}$ of image f obtained from blurred image g minimizes the averaging measure (second-order derivative).

3. Spatial Domain Processing, State Space Method: Inverse filtering, Wiener filtering and constrained inverse faltung all recover the image in the frequency domain. This requires that we perform the Fourier transform and inverse Fourier transform of the image. Even if we have a fast method of calculating the fast Fourier transform and the fast Hadamard transform, we still need large amounts of memory and a large number of operations, which is not conducive to real-time processing. Reference 5 [not reproduced] describes the use of a dynamic state space model which does not need to be converted into the frequency domain, for direct processing in the spatial domain. It uses the digital computer's suitability for recursive operations, effects a great saving of operations and memory, and is suitable for real-time processing. The dynamic model can also be combined with the Karman filter and self-adaptive filter, to perform recovery processing on blurred images which contain noise interference.

Comparison of the State Space Method of Recovering a Motion-Blurred Image with Frequency Domain Inverse Filtering (Carried Out With the Fast Fourier Transform

To perform an FFT on the linear image with N elements and filter requires $4N \log_2 N + N$ multiplications; the state space method requires only $N (m + 3)$ multiplications (where m is the number of motion-displace image elements). If $N = 256$ and $m = 10$, the linear image can be recovered with 5,120 fewer multiplications.

Investigation of the image recovery method has progressed very rapidly in recent years and has achieved many results, for example, the maximum probability and maximum entropy methods, and the shortest dispersion inverse faltung method. In addition, image recovery methods for spatially variable systems have been proposed.

8480
CSO: 8111/0852

APPLIED SCIENCES

NEW COSMIC DUST DISCOVERED IN ATMOSPHERE, ANCIENT STRATA

Beijing GUANGMING RIBAO in Chinese 16 Jun 81 p 2

[Article by Xiao Zhong [2556 0112]: "China Discovers Cosmic Dust in Ancient Strata and in Atmospheric Dust"]

[Text] After China discovered deep-sea cosmic dust in 1980, recently scientists at the Institute of Petroleum Exploration and Development of the Ministry of Petroleum Industry also discovered characteristic tiny spheres in atmospheric dust. The Nanhai Institute of Petroleum Geology has discovered a similar substance in ancient strata in China. Preliminary identification indicates that they are interstellar cosmic dust.

This is the first time in China that cosmic dust has been gound in ancient strata and in atmospheric dust. This discovery has provided new types of specimens for China's research into cosmic matters in addition to meteors, moon rock and deep sea cosmic dust. It opens up a new realm for China's research into ancient strata and modern cosmic matter.

This cosmic dust consists of minute spherical particles ranging from 0.02 mm to 2 mm in diameter. Under a microscope, one of the two types of specimens discovered recently has a surface with the appearance of black paint. Some have smooth surfaces and look like shiny spheres, while others have rough surfaces with a recognizable pattern. This type of sphere has a fairly strong magnetism and is quite brittle. Energy spectroscopic analysis shows that it consists mostly of iron. It is generally referred to as cosmic dust or a magnetic sphere. The other type of specimen is a transparent or translucent glassy sphere with a wavy or smooth surface. A local crystalline or glassy fiber structure can also be seen. Energy spectroscopic analysis shows that the major ingredient is silicon. It is probably a microscopic glassy meteor. Using a scanning electron microscope, fine structures on the surface of this type of sphere can be observed; a microscopic structure of the interior and an extremely thin shell can also be clearly seen. The variety of surfaces and the interior characteristic appearance are formation records of the cosmic dust, bringing us valuable information of the universe. This can help us to understand and explore the complex physical and chemical processes of cosmic matter as it enters the atmosphere and it can also serve as an important basis for cosmic dust identification.

Cosmic dust is increasingly important in the research in geology, astronomy and space science. The cosmic dust discovered in China's ancient strata and atmosphere provides valuable material specimens for investigating the age of ancient strata and contemporary cosmic matters. The discovery of microglass meteors in China provides important new data for the study of the world distribution and formation of glass meteors.

9698
CSO: 4008/387

ELECTROFLOTATION OF LEAD-ZINC ORE DESCRIBED

Beijing YOUSE JINSHU [NONFERROUS METALS] in Chinese No 2, 1981 p 36

[Article by Liu Jingwen [0491 5427 2429] (Changhua Lead-Zinc Mine, Guangdong)]

[Text] This paper describes the research work and production practice of separation of a lead-zinc sulphide ore by electroflotation.

The ore treated was a polymetallic sulphide ore. The ore contained 2 percent Pb, 4 percent Zn and a certain amount of pyrite, the principal minerals being galena, sphalerite and pyrite. Galena amounted to 80 percent in minus 0.06 mm size fraction, dissoluting pyrite and sphalerite.

The plant adopted a differential flotation flowsheet to treat this type of ore before the use of electroflotation. The metallurgical results achieved were as follows: the grade of lead concentrate 45.64 percent (as pyrite contained a certain amount of gold and no separation was made, thus having a low grade of lead concentrate), lead recovery 82.81 percent; zinc concentrate assaying 59.98 percent, and recovery 81.88 percent.

Flotation research by means of several types of electrodes showed that the lead-zinc complex mineral was separated successfully through the depression on zinc mineral, without the use of regulators, depressants and other reagents. The effect of copper-carbon was better, zinc-carbon electrode being second. Electroflotation could also be used for separating copper-sulfur (pyrite) bulk concentrate. The bulk concentrate contained lead from 29.47 percent to 32.56 percent. The content of the lead concentrate after separation was between 54.60 percent and 57.06 percent, the lead recovery being up to 97 to 98 percent.

The flowsheet of differential flotation by use of zinc-carbon electrode at a plant has brought about good results in treating the above ore. The lead concentrate grade increased to 41.33 percent (no separation of pyrite; if separated, 60 percent could be obtained), with a recovery of 87.29 percent; zinc concentrate containing 59.85 percent Zn, with a recovery of 83.28 percent.

The above results show that the electroflotation method is effective in separating the lead-zinc mineral. The metallurgical results achieved are equal to or slightly higher than those by using flotation reagents. Sodium carbonate, sodium sulphite, zinc sulphate and other reagents can be saved. The amount of xanthate and copper sulphate can be reduced by 35 percent and 60 percent respectively. The electroflotation technique is of benefit to a plant.

CSO: 4008/409

NATIONAL SYMPOSIUM ON TUNGSTEN RESEARCH HELD

Beijing YOUSE JINSHU [NONFERROUS METALS] in Chinese No 2, 1981 p 90

[Text] China is rich in tungsten ore resources; nevertheless, for many years China has exported mainly tungsten concentrates, and still has to import some tungsten products. To discuss the problems of improving the export product structure and making full use of the abundant tungsten resources, a National Symposium on Tungsten Research was held in Beijing on 4-8 November 1980, sponsored by the Ministry of Metallurgical Industry.

Attendants at this meeting were 42 experts concerned, coming from 20 organizations in tungsten ore beneficiation, metallurgy and metal working fields. Eleven papers were presented, involving detailed comparison and analysis of tungsten resources, production and consumption both at home and abroad; discussion on the main technical problems in tungsten ore beneficiation, metallurgy and metal working; drawing up a scientific research program and making some important suggestions of the management system, price and so on.

It is believed that since the foundation of PRC, the tungsten industry has been rapidly developed so the tungsten concentrate production of China is ranked first in the world; simultaneously, the metallurgy and metal working industries have also gained remarkable progress, so most of tungsten products are now self-sufficient. China is in all conditions to carry out an intensive research work on tungsten products to improve quality, increase variety and gradually reform the structure of exported products, and consequently to make better use of its resources.

The symposium indicated that the main reason having prevented China from full utilization of its tungsten resources just lies in the less developed science and technology of tungsten metallurgy and working. Furthermore, a series of factors, such as tungsten resources control, its concentrate production, marketing and price, and its consumption structure also have significant effect on the issue.

The symposium suggested to establish a national tungsten society in order to exchange experience, coordinate management policies and acquire technical and economic information about tungsten production abroad.

The scientific research items raised by various establishments at the symposium were collected, discussed and fixed up. The subjects of ore beneficiation and metallurgy were mainly: improvement of tungsten concentrate quality and establishment of new standards for the concentrates, reasonable metallurgy technology for tungsten middling slimes, treatment of intergrown sheelite-wolframite slimes, treatment of tungsten bearing limonite and magnetite ores, new chlorinating metallurgy technology, and steelmaking with direct use of high quality sheelite concentrate.

CSO: 4008/409

FIRST SYMPOSIUM OF TECHNOLOGICAL MINERALOGY HELD

Beijing YOUSE JINSHU [NONFERROUS METALS] in Chinese No 2, 1981 pp 87-89

[Text] The First Symposium of Technological Mineralogy was held by the Mineral Processing Academic Committee of Chinese Metal Society, and the Protection and Comprehensive Utilization of Mineral Resources of Chinese Geological Society in Emei, Sichuan Province on 20-25 November 1980. There were 148 members from 69 units present at the symposium.

The following seven papers were read out at the symposium:

1. Development of Technological Mineralogy by Cheng Xiao (Principal engineer, director of research section, Mining and Metallurgical Research Institute, Ministry of Metallurgical Industry)

2. Crystallization-Differentiation of Copper-Bearing High Nickel Matte From Jinchuan Plant by Ge Shuhua (Associate researcher of Research Institute of Comprehensive Utilization of Minerals)

3. Theory and Study Method of Crystal Fracture by Xing Yongqing (Engineer of Beijing Mining and Metallurgical Research Institute)

4. Mineralogical Research of Difficult Treated Violarite by Cheng Yukun (Engineer, director of research section, Baiyin Mining and Metallurgical Research Institute)

5. Application of Electronic Probe and Ionic Probe in Mineralogical Research by You Junfu (director of Shanghai Measuring and Testing Institute)

6. Approach of Characteristics of Lean Ore of No 1 Mining Section of Jinchuan Open Pit and Its Processing Method by Hu Xigeng (Professor of Central-South Mining and Metallurgical Institute)

7. Use of Mineralogy in Metallurgical Process by Tian Fuchun (Engineer of Beijing Mining and Metallurgical Research Institute)

At the group meetings, 97 papers were read out, from which 51 papers related to mineral processing; 21 papers to metallurgy; 25 papers to research methods and techniques.

Papers related to mineral processing mainly include:

1. Development of Technological Mineralogy of Beneficiation by Liu Xinghua (Lecturer of Xian Metallurgical Architecture Institute)

2. Effect of Mineral Composition Property of Raw Ore in Qidashan Iron Mine on Mineral Processing Technology by Xia Yurong and Yuan Ruihua (Assistant engineers of Anshan Research Institute of Metal Mines)

3. Internal Relations of Mineral Composition of Ore From Jinchuan Open Pit With the Reasons of Its Difficult Treatment by Zhou Mangeng (Assistant engineer of Research Institute of Comprehensive Utilization of Minerals)

4. Research and Practice of Technological Mineralogy of Vein Tungsten Ore by Xu Deqing and Wu Zilan (Assistant researchers of Jiangxi Nonferrous Metallurgical Research Institute)

5. Features of Oxide-Copper Iron Ore of Tonglushan Mine and Its Effects on Industrial Utilization by Dai Zaisheng (Engineer of Changsha Nonferrous Metallurgical Design Institute)

6. Research of Effect of Lead-Zinc-Pyrite Ore Property of Tanshan, Suzhou on Its Processing by Ning Renzu and Yu Jinqi (Engineers of Laboratory of Jiangsu Geological Bureau)

7. Research of Features of Fracture Zone Ore of Jinduicheng Molybdenum Mine and Factors of Difficult Treatment by Zhou Guohua (Lecturer of Xian Metallurgical Architecture Institute)

Papers related to smelting mainly include:

1. Research of Technological Mineralogy of Flue Accretion by Luo Shaohong (Engineer of Baiyin Mining and Metallurgical Research Institute)

2. Research of Mechanism of Phase Charge of Roasting of Vanadium-Bearing Minerals by Li Xingzhi and Zhang Fa (Engineers of Baiyin Mining and Metallurgical Research Institute)

3. Research of Crystal Structure Change of Oxidizing Reaction Process of Panzhihua Grained Ilmenite by Huang Jishang, Xiao Yaqin and Jiang Shuzhi (Assistant researchers of Mining and Metallurgical Research Institute, Ministry of Metallurgical Industry)

4. Approach of Mineral Composition of Congelation of High-Temperature Electric Furnace for Smelting Nickel Ore and Its Effects on Nickel-Bearing slag by Zhou Guizhen (Engineer of Research Institute of Jinchuan Nonferrous Metal Corporation)

5. Research of Phase Charge of Vanadium Extraction From Vanadium-Bearing Steel Slag by Sodium Carbonate roasting by Liu Xiouqing (Engineer of Geological Research Institute of Chemical Mines, Ministry of Chemical Industry)

6. Growth of Calcium Ferrite in Sinter and Metallurgical Feature by Tang Jingyu (Engineer of Anshan Research Institute of Ferrous Metal Mines)

7. Research of Relations of Heap-Baurite Feature With Aluminum Melted Property by Wang Shuyu (Engineer of Guangxi Metallurgical and Geological Research Institute)

Papers related to research method and technology mainly include:

1. Allowance Measurement About Particle Size Distribution by He Tong (Assistant researcher of Research Institute of Chemical Metallurgy, Academia Sinica)

2. Research of Laser Microspectral Analysis--A New Quantative Method of Heavy Sand Minerals by Li Weihua and Duan Zhiran (Engineers of Measuring and Testing Institute of Rock and Ore, Academy of Geological Sciences)

3. Value K Measurement of Magnetite Content of Samples by Zhang Weishai (Lecturer of Beijing Iron and Steel Institute)

4. Magnetite Measuring Meter by Huang Daqiu (Mine Research Institute, Wuhan Iron and Steel Company)

5. Research Methot of Technological Mineralogy of Platinum Family Element by Zhou Xuesui, Liu Yunxian and Zou Kaixun (Assistant engineers of Research Institute of Comprehensive Utilization of Minerals)

6. X-ray Diffraction of Single Microsize Powder by Tang Renwei and Yang Yunqi (Engineers of Beijing Mining and Metallurgical Research Institute)

This symposium reflected the development in all aspects of mineralogical research in China of late over 10 years. In order to coordinate the research of mineral processing and smelting process, the division of ore process types, the mineral composition and structure of various kinds of ores, distribution and occurrences of value and harmful elements, as well as mineralogical features, such as magnetics, electricity and surface property, and so on, of a variety of ores have been investigated, so that providing the basis for designing reasonable flowsheet of beneficiation. Many papers dealt with the relations of mineral recrystallization and phase change in sintering process with the strength of sinters, the relations of slag types with metal losses, the relations of crystal growth with heat preservation time, the relations of copper segregation and roasting with metallurgical results, the research of thermal stability of synthetic minerals and crystal charge and meltability of natural mineral after heat treatment, research of mineral composition of furnace charge and built-up of various positions in smelter. These researches are of actual significance for improving the operation control of smelting process.

China has developed rapidly on the methods and techniques of mineralogical research in recent over ten years. The application of electronic probe and ionic probe has been realized. The mineral quantitative determinations, such as X-ray diffraction, X-fluorescene, laser spectrum, and so on have been widely used. The new trends of micro-size content determination, value K measurement and so on have been emerged. The development of mineralogical research in depth and range leads to get a deeper understanding of mineral behavior in process, so that providing more data for improving and perfecting the process.

The Second Symposium of Technological Mineralogy was decided at this symposium to be held in 1982.

CSO: 4008/409

APPLIED SCIENCES

HEAT TREATMENT FOR PROCESSED BERYLLIUM BRONZE DESCRIBED

Beijing JINSHU RECHULI [HEAT TREATMENT OF METALS] in Chinese No 4, 1981 pp 1-10

[Article by Zhou Shanyou [0719 0810 0147] of the Shanghai Jiaotong University: "Heat Treatment of Beryllium Bronze"]

[Text] Beryllium bronze is a typical precipitation-hardening copper alloy. This kind of alloy possesses good cold processing and forming properties in the soft state after solid solution treatment. It can be formed into complex parts of all different shapes. Afterward, when subjected to age-hardening under appropriate temperatures, it can undergo intense precipitation-hardening. Because this type of alloy has good comprehensive properties--besides high strength, elasticity, hardness, wearability and fatigue resistance, it also retains the superior qualities of copper alloys of thermal conductivity, electrical conductivity, corrosion resistance, cold tolerance, and nonferrous magnetism, and it does not produce sparks when being blasted--the uses of this type of alloy are expanding daily and it has already become a very important metallic material in the precision instruments and meters manufacturing industry, electronics industry and electrical appliances industry. However, the many superior properties of beryllium bronze can only be obtained through appropriate heat treatment. Correct heat treatment is the key to improving the quality of beryllium bronze parts.

Beryllium bronze can be divided into two categories: cast beryllium bronze and processed beryllium bronze (also called deformed beryllium bronze). This article will deal only with the heat treatment for processed beryllium bronze.

1. Chemical Composition of Beryllium Bronze

The numbers and chemical composition of processed beryllium bronze produced in our nation are listed in Table 1.

As shown by the binary phase diagram of the copper-beryllium alloy illustrated in Diagram 1, the degree of solid solution of beryllium in solid copper visibly lessens as the temperature drops. This enables beryllium bronze to strengthen in age-hardening after solid solution treatment (quenching).

Although binary beryllium bronze possesses a high capacity to harden by aging, it easily undergoes discontinuous precipitation and over aging, affecting the effect of hardening by heat treatment. For this reason, industrial beryllium bronze almost always contains traces (0.2%-0.5%) of nickel or cobalt to overcome this shortcoming. Furthermore, the addition of traces of nickel or cobalt also hinders the enlargement of crystal grains during the quenching process of the alloy. This helps to produce better properties in the alloy after heat treatment. Diagram 2 shows the effect of traces of nickel and cobalt upon the age-hardening curve of the copper-beryllium alloy.

Table 1. Chemical Composition of Processed Beryllium Bronze (YB147-71)

(1)	(2)												
	(3)				(4)								
	(5)	(6)	(7)	(8)	(9)	(10)	(11)	(12)	(13)	(14)	(15)	(16)	(17)
QBe2	1.9~2.2	0.2~0.5	—	(18)	0.15	0.15	0.005	—	0.15	[illegible]	[illegible]	[illegible]	0.5
QBe2.15	2.0~2.3	—	—	(18)	0.15	0.1	0.01	0.02	0.4	0.002	[illegible]	0.08	1.2
QBe1.7	1.6~1.85	0.20~0.40	0.10~0.25	(18)	0.15	0.15	0.005	—	0.15	—	—	—	0.5
QBe1.9	1.85~2.10	0.20~0.40	0.10~0.25	(18)	0.15	0.15	0.005		0.15				0.5

Key:

1. Number of alloy
2. Chemical composition, %
3. Main composition
4. Impurities, less than
5. Beryllium
6. Nickel
7. Titanium
8. Copper
9. Silicon
10. Aluminum
11. Lead
12. Phosphorus
13. Iron
14. Bismuth
15. Nickel
16. Magnesium
17. Total
18. Remaining

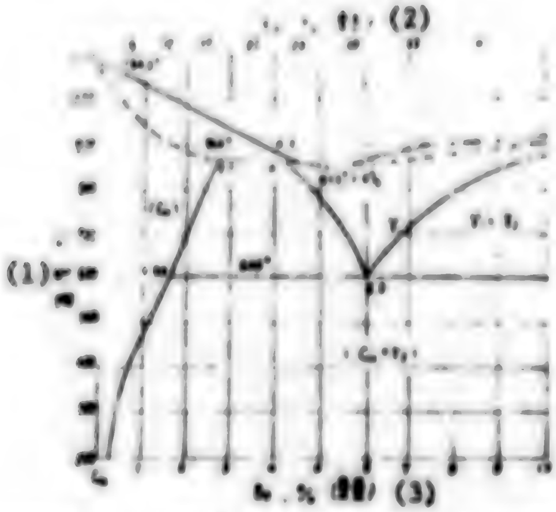

Diagram 1. Cu-Be Binary Phase Diagram (1)

Key:

1. Temperature
2. Atom
3. Weight

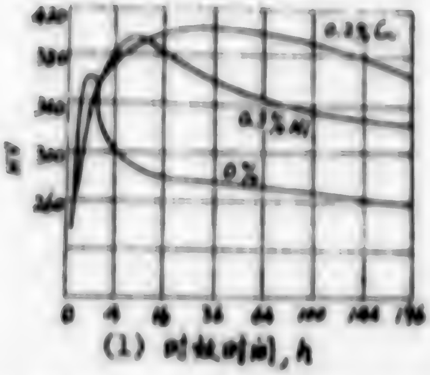

Diagram 2. Effect of traces of nickel and cobalt upon the age-hardening curve of beryllium and copper alloy (containing 1.9%-2.15% beryllium). The alloy was age-hardened at 300° C after quenching at 750° C. (2)

Key:

1. Duration of age-hardening, h

In some beryllium bronze, traces (0.10%-0.25%) of titanium are added. This refines the crystal grains after casting, heat processing and quenching. It also hinders discontinuous precipitation and the occurrence of crystalline boundary reactions and allows a lower content of beryllium and nickel without reducing the mechanical properties of the alloy. This reduces the number of brittle and hard γ_1 phases remaining in the alloy after quenching the alloy, thus improving the evenness of the organization of the alloy so that its strength against fatigue is higher, it has a better elastic stability and a small elastic delay after age-hardening.

II. Quenching Beryllium Bronze

Beryllium bronze bands, wires, strips, rods and similar pressed semifinished products are mostly supplied in a quenched state (soft state) or cold hardened state after quenching (semihard state, hardened state). Materials in these states (especially soft materials) frequently can be directly cold formed into suitable shapes as parts. At the same time, already formed parts can be directly precipitated and hardened by age-hardening. Therefore, unless special needs have to be satisfied, such as softening the material for further cold forming or remaking pieces that have been mistakenly age-hardened, generally factories manufacturing beryllium bronze parts do not quench beryllium bronze.

Solid solution treatment of beryllium bronze is also called quenching. It includes the processes of heating the material or the work piece to an appropriate temperature and keeping it at that temperature, then quickly quenching it in cold water for cooling. Quenching solidifies the solution of the rich beryllium phase in the basic material of beryllium bronze and thus obtains an oversaturated solid solution material which can be precipitated and hardened, and because the temperature for quenching beryllium bronze is higher than the recrystallization temperature, the material processed and hardened can be softened for further cold forming or deformation into the needed shape.

When quenching beryllium bronze, the heating temperature, the duration of temperature retention, and quenching and cooling must be carefully controlled to assure that the material will possess the best properties after age-hardening.

The heating temperature in quenching must be appropriate. If the heating temperature is too high, the crystal grains will be too coarse (overheating) and will even partially melt (overburning). Large and coarse crystal grains will damage the forming ability and the mechanical properties of the material. Overburning will cause the material to become brittle and unusable. If the heating temperature is too low, the rich beryllium phase cannot fully solidify as a solution in the crystal grains of the base material and the distribution will be uneven. This will lower the precipitation and hardening abilities of the material and during the course of age-hardening, discontinuous precipitation and crystal boundary reactions will easily occur, thus reducing the material's elastic stability and increasing elastic delay. The appropriate quenching temperature should enable the rich beryllium phase in the material to fully solidify as a solution in the basic material crystals and to be distributed evenly, and at the same time, the material should possess fine crystal grains after quenching. The dimension of the crystal grains of beryllium bronze materials after quenching should not surpass the numerical values listed in Table 2. The recommended quenching temperatures for beryllium bronze are listed in Table 3.

Table 2. Dimensions of Crystal Grains of Beryllium Bronze Material Required After Quenching (3)

(1) 材料厚度，(mm)	(2) 最大平均晶粒尺寸，(mm)
(3) 大于0.25至0.76	≤0.035
大于0.76至2.29	≤0.045
大于2.29至4.78	≤0.060

(4) 注：[illegible]

Key:

1. Thickness of material (mm)
2. Largest average dimension of crystal grains (mm)
3. Greater than ____ to ____
4. Note: Measured on the buffed surface parallel to the rolled direction and perpendicular to the surface of the material.

Table 3. Some Recommended Quenching Temperatures for Beryllium Bronze (4)

(1) 合 金 牌 号	(2) 淬火加热温度，(°C)
QBe2	780～800
QBe1.9	770～790
QBe1.7	770～790

Key:

1. Number of alloy
2. Quenching temperature

The duration of temperature retention during quenching of beryllium bronze should be sufficient to allow the rich beryllium phase to fully solidify in solution, and at the same time, it should not cause the crystal grains to enlarge intensely. For rods, strips and work pieces with thicker cross sections, the duration of temperature retention should be calculated on the basis of one hour per 25 millimeters of cross sectional thickness. For thin plates and bands and thin work pieces, the recommended durations of temperature retention are listed in Table 4.

Table 4. Duration of Temperature Retention During Quenching of Thin Plates, Bands and Thin Work Pieces of Beryllium Bronze (5)

(1) 材料厚度，(mm)	(2) 保温时间 (min)
(3) 0.13以下	2~6
0.13~0.25	3~9
0.25~0.76	6~15
0.76~2.30	10~30

Key:

1. Thickness of material (mm)
2. Duration of temperature retention (min)
3. Less than 0.13

At the end of temperature retention during quenching, the beryllium bronze work pieces are taken out of the furnace and immediately quenched in water of 35° C as soon as possible. Any delay will cause the rich beryllium phase to separate out at the crystal boundary. This will not only reduce the ability of the material to precipitate and harden, but it will also promote the occurrence of discontinuous precipitation and crystal boundary reactions during age-hardening, thus reducing the material's elastic stability and increasing elastic delay. When quenching, the maximum duration of quenching allowed is determined by the dimensions of the work piece, the total weight of the work pieces quenched together and the temperature and velocity of the flow of surrounding air. To determine whether quenching is effective or not, the quenched work pieces should be subjected to metallic phase analysis and their mechanical properties should be tested.

When beryllium bronze is quenched in air or in oxidizing furnace gases, the surface will oxidize to form an oxidized layer. The oxidized layer on the various types of beryllium bronze listed in Table 1 is continuous and tough. Although it does not visibly affect the mechanical properties of the material after precipitation-hardening, it is abrasive, and during cold forming it will cause serious abrasive damage to tools and molds. To avoid surface oxidization, beryllium bronze should be quenched in a vacuum heating furnace or in heating furnaces using dry and sulphurless cracked ammonia gas, hydrogen or protective gas with a dew point not higher than -40° C used for cracking city coal gas to obtain a shine in heat treatment. If conditions do not permit heat treatment to obtain a shine, quenching can also be done in an electric furnace or a coal gas furnace. Then, the black oxidized layer can be removed by acid washing, which will be described later on in this article.

It must be pointed out that beryllium bronze cannot be quenched in a salt bath furnace because within the quenching temperature range, most melted salt will rapidly cause corrosion among the crystals and the removal of beryllium on the surface of the material, thus seriously lowering the properties of the material.

III. Age-Hardening of Beryllium Bronze

The main purpose of age-hardening of the soft, semihard and hard quenched beryllium bronze material and parts formed from it is to produce precipitation-hardening. However, using different aging temperatures and durations of aging can produce combinations of different strengths, hardness, plasticity, electrical conductivity, hitting toughness and delayed elasticity in the alloy after aging.

The properties of beryllium bronze after aging, such as strength, hardness, plasticity, and electrical conductivity, are mainly determined by the parameters such as the alloy's content of beryllium, aging temperature, duration of aging and cold processing after quenching. In addition, the size of the crystal grains of the material, content of impurities, the dimension of the rich beryllium phase remaining after quenching and distribution also affect the properties after aging.

Diagram 3 shows the effects of aging temperature, duration of aging and cold processing after quenching upon the QBe 2 (containing 1.9% Be, 0.2% Ni) alloy after aging. It can be seen from Diagram 3 that: 1) aging can improve the strength, hardness and electrical conductivity of the alloy to different degrees while plasticity drops; 2) cold processing after quenching can produce a higher strength and hardness after aging while plasticity and electrical conductivity of the alloy after aging are lower than those of alloys not cold processed; 3) improving the aging temperature can hasten the progress of aging: the peak value strength of the constant temperature aging curve can be obtained within a shorter aging period of the material but the numerical value drops as the aging temperature rises, while on the other hand, improving the aging temperature can also produce over aging of the material during the course of aging; 4) cold processing after quenching can also hasten the progress of aging, enabling the material to reach the peak value strength within a shorter aging period and at the same time enabling the material to over age even earlier.

The commonly used aging treatment of beryllium bronze can be divided into two types: 1) standard low-temperature aging; 2) short-period high-temperature aging.

Standard low-temperature aging is to age the material under temperatures of 315°-343° C for 2-3 hours. Quenched alloys with a higher content of beryllium (such as semihard and hard QBe 2, QBe 1.9) can be aged at a lower aging temperature and in a shorter aging time. Alloys with a lower beryllium content and not quenched (such as soft QBe 1.7) can be aged at a higher aging temperature and for a longer aging time. Standard low-temperature aging is easy to control, the demand for aging temperature and aging time is not strict (aging temperature needs only to be controlled within ±5° C), and compared to other types of aging, the maximum strength and hardness can be obtained. This type of aging is recommended for use to produce work pieces that require maximum strength and hardness but do not require other special properties. In addition, when beryllium bronze work pieces of large cross sections require aging and hardening, to assure that the entire cross section of the work piece can be evenly heated and aged, this type of standard low-temperature aging is also required. Table 5 compares the properties of two kinds of beryllium bronze before and after standard low-temperature aging.

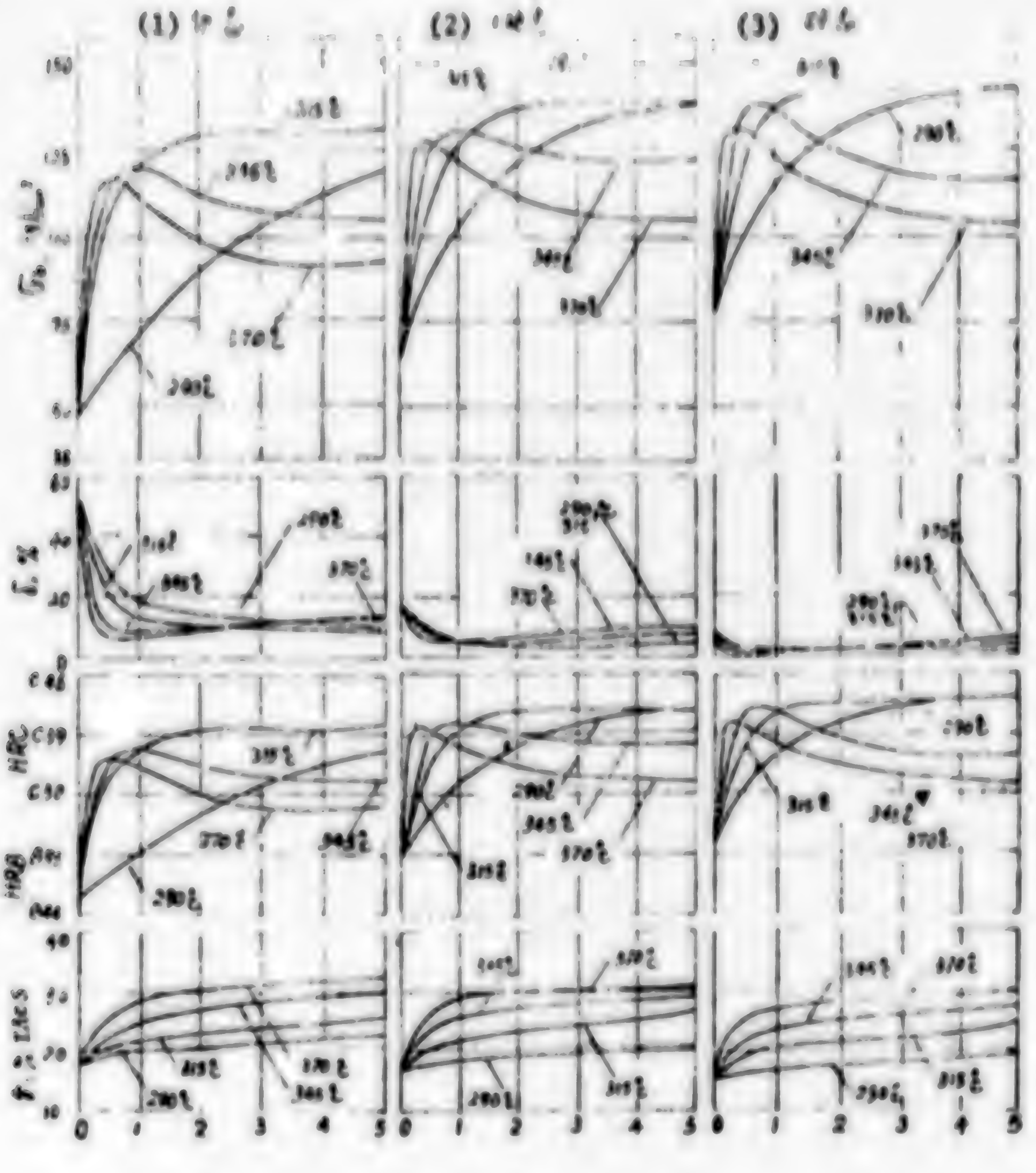

Diagram 5. The Effect of Aging Temperature, Aging Time and Cold Processing Upon the Properties After Aging of Quenched QBe 2 Alloy (containing 1.9% Be, 0.2% Ni) (6)

Key:

1. Soft State
2. Semihard State
3. Hard State

Table 5. Comparison of the Properties of Two Kinds of Beryllium Bronze Before and After Standard Low-Temperature Aging (7)

(1)		(2) (3)	(4)	(5)	(6)	(7)	(8)	(9)
[illegible]								
(10)	(14)	(17)		42.2~54.8	14.3~24.6	[illegible]	HRB 45~78	17~19
	(15)	(17)		58.0~70.3	47.7~65.3	5~25	HRB 88~96	15~17
	(16)	(17)		70.3~81.6	56.2~78.7	2~8	HRB 96~102	15~17
	(14)	315	3	110~133.6	98.4~123	4~10	HRC 32~40	22~25
	(15)	315	2	130~147.6	112.5~133.6	2~5	HRC 39~44	22~25
	(16)	315	2	133.6~151.1	112.5~144.1	1~4	HRC 40~45	22~25
(11)	(14)	(17)		42.2~59.8	14~21.1	35~60	HRB 45~85	17~19
	(16)	(17)		60.8~91.4	52.7~73.8	10~20	HRB 88~103	15~17
	(14)	315	3	116~133.6	101.9~123	3~10	HRC 36~41	22~25
	(16)	315	2	126.6~151.2	106.5~140.6	2~5	HRC 39~45	22~25
(12)	(14)	(17)		40.8~54.8	14.1~21.6	35~45	—	17~19
	(15)	(17)		77.3~94.9	63.3~77.3	4~10	—	15~17
	(14)	315	3	116~133.6	101.9~123	3~8	—	22~25
	(15)	315	1 1/2	133.6~151.2	123~140.6	1~3	—	22~25
QBe1.7(1.7%Be, 0.2% Ni)								
(13)	(14)	(17)		42.2~54.8	17.6~24.6	35~60	HRB 45~78	17~19
	(15)	(17)		59.8~70.3	45.7~63.3	5~25	HRB 88~96	15~17
	(16)	(17)		70.3~84.4	56.2~77.3	2~8	HRB 96~102	15~17
	(14)	315	3	112.5~130.9	87.9~116	4~10	HRC 34~40	22~25
	(15)	320	2	126.6~140.6	98.4~126.6	2~5	HRC 38~42	22~25
	(16)	320	2	130.1~144.1	109~133.1	2~5	HRC 38~43	22~25

(18) ① [illegible] 1.27mm.
(19) ② [illegible] HRB [illegible] HRC [illegible] 1.02mm [illegible].

Key:
1. State of material before aging
2. Standard low temperature aging
3. Temperature
4. Time
5. Tensile strength
6. Yielding strength
7. Extension
8. Rockwell hardness (2)
9. Electrical conductivity
10. Band material
11. Rod and strip
12. Wire (1)
13. Band
14. Soft
15. Semihard
16. Hard
17. Not aged
18. (1) Diameter of the wire is greater than 1.27 mm.
19. (2) The numerical values of Rockwell hardness HRB and HRC are correct only when the thickness of the metal is ≥ 1.02 mm.

Short-time high-temperature aging is done under 350°-380° C for 15-90 minutes. Cold processed alloys with a higher content of beryllium are aged at lower aging temperatures and for a shorter aging time. Alloys containing less beryllium and not cold processed are aged at higher aging temperatures and for a longer time. Because this type of aging process can eliminate internal stress caused by quenching and cold deformation before aging to a greater degree, it can produce a better capability to resist fatigue, zero wander and relaxation in the material, and it can also make the work piece better accept and retain the shape fixed by the fixture during aging in the fixture. In addition, this type of aging process can also produce a higher electrical conductivity, plasticity and modulus of elasticity in the material, and it can shorten the cycle of heat treatment and improve the production rate.

The properties produced by short-time high-temperature aging and their relationship to the duration of aging are shown in Diagram 4. Under the aging temperature (350° C) used, treatment No 1 can produce the highest hardness and wearability. Treatment No 2 can produce the highest elastic stability and is used to make springs and diaphragms that have strict requirements for good resistance to zero wander, delay and relaxation. Treatment No 3 can eliminate internal stress well so that the work piece can be shaped well by the fixture to achieve the best dimensional control.

When beryllium bronze undergoes short-time high-temperature aging, the control over aging temperature and aging time is very strict. Aging temperature is best controlled within ±3° C. Work pieces with large cross sections or large amounts placed in the furnace cannot be evenly heated and aged because of the "mass effect." Therefore, they are not suited for short-time high-temperature aging. Short-time high-temperature aging is generally suited for treating relatively thin or small work pieces made of band or wire materials as well as work pieces that require strict control over the shape and dimensions during aging in the fixture. At the same time, the best aging temperature and aging time should be determined by experiment according to the demands of the properties of the work pieces.

The properties of the QBe 2 (containing 1.9% Be, 0.2% Ni) beryllium bronze band after short-time high-temperature aging are listed in Table 6.

The aging of beryllium bronze is generally conducted in an air furnace equipped with forced air circulation or a salt bath furnace to assure that the temperature fluctuation during the process of temperature retention during aging is not greater than 5° to 3° C. Aging to obtain a shine in a protective atmosphere is generally not needed because after aging in the air furnace or the salt bath furnace, an hermetic oxidized film forms on the surface of the work piece and it does not affect the mechanical and physical properties. At the same time, when a clean external surface is required or when a clean surface is required in later tin welding, silver welding, or electroplating operations, this oxidized film can be easily removed by acid washing.

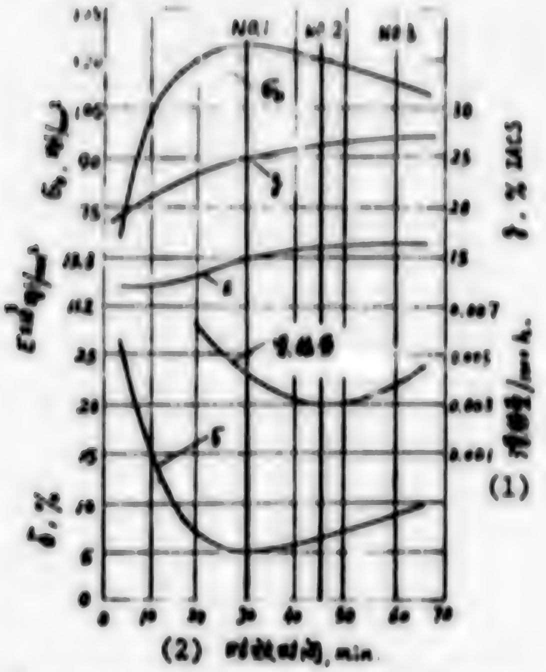

Diagram 4. Variation of Properties of Soft QBe 2 (containing 1.9% Be, 0.2% Ni) Beryllium Bronze Band After Aging for Different Lengths of Time (8)

Key:

1. Amount of wander
2. Aging time

Table 6. Properties of QBe 2 (containing 1.9% Be, 0.2% Ni) Beryllium Bronze Band After Short-Time High-Temperature Aging (9)

(1)	(2) (min)	(3) σ_b (kgf/mm²)	(4) $\sigma_{0.2}$ (kgf/mm²)	(5) δ (%)	(6) γ (%IACS)	(7) (kgf/mm²)	(8) E (kgf/mm²)
(9)	(10)	47.5	25.3	48	18.0	23.1	11601
	5	87.2	71.0	18	19.5	—	12304
	15	121.6	107.6	10	22.0	—	12655
	30	120.3	107.9	6	23.0	—	12655
	60	126.0	107.6	5	25.5	26.0	13007
	120	122	106.2	6	28.0	—	13007
(11)	(10)	61.5	58.0	17	16.0	23.2	11952
	5	130.8	113.2	3	21.0	30.2	12655
	15	133.6	119.0	2	23.0	30.9	13007
	30	135.3	120.2	2	24.5	30.9	13007
	60	130.4	112.6	2	25.0	30.2	13007
	120	122.3	105.8	3	26.0	29.1	13007
(12)	(10)	74.5	70.3	5	15.0	27.4	12304
	5	137.6	114.6	3	18.0	—	12655
	15	138.5	121.6	2	21.0	—	13007
	30	133.0	119.5	1	24.5	32.3	13358
	60	132.2	112.5	1	26.5	—	13358
	120	126.6	111.1	2	27.5	—	13358

Key:

1. State of material before aging
2. Aging time under 370° C
3. Tensile strength
4. Yielding strength
5. Extension
6. Electrical conductivity
7. Strength against fatigue (10^7 cycles)
8. Modulus of elasticity
9. Soft
10. Not aged
11. Semihard
12. Hard

Rapid and even heating of beryllium bronze in the salt bath furnace can produce good results at any aging temperature. At the same time, short-time high-temperature aging and aging of pieces fixed in the fixture can provide special benefits. The recommended content of the salt bath is 40% to 50% sodium nitrate, the rest being sodium nitrite and potassium nitrite. The melting point of this kind of mixed salt is about 143° C. Besides being used for aging beryllium bronze, it can also be used for annealing and removal of stress in beryllium bronze.

Before the work piece is placed in the furnace or the salt bath for heating, it should be cleaned and it should not contain any water. Any organic matter, such as tallow, will react violently with the fused nitrate-nitrite and even cause an explosion. To obtain the best results, the salt bath for beryllium bronze should be kept clean and it should not be used for other materials (such as steel). After the work piece is removed from the salt bath, it should be thoroughly cleaned to wash away any traces of salt. The following washing operation produces good results: 1) quenching the work pieces in cold water; 2) washing the work pieces in hot detergent solution; 3) washing in hot water; 4) drying.

IV. Other Heat Treatments

1. Softening and Annealing Below the Critical Point

Intermediate softening and quenching between the two cold deformations of beryllium bronze can be replaced by annealing under 550 ±10° C retained for 5 to 7 hours. This kind of softening and annealing below the critical point can produce recrystallization in the basic material of the solid solution after cold deformation, forming new refined crystal grains without strain, and it can aggregate and spheroidize the precipitation phase. Beryllium bronze subjected to this type of annealing possesses good cold processing properties. For example, in actual production conditions, a band of QBe 2 with a width of 260 mm annealed for 7 hours under 550° C can be cold rolled from a thickness of 5 mm to 2.5 mm, and it can be further cold rolled from 2.5 mm to 1.2 mm and even to 0.78 mm in thickness after a second annealing the same way. But it should be pointed out that compared to quenching, the strength and hardness obtained by such softening and annealing below the critical point are higher and the plasticity is lower (as shown in Table 7). Also, alloys subjected to such softening and annealing do not possess precipitation-hardening ability like alloys subjected to quenching. Therefore, when a work piece requires the lowest strength and highest plasticity after softening during cold deformation and when it requires a precipitation-hardening ability after softening, softening by quenching should be used.

2. Annealing to Remove Stress

Annealing to remove stress can greatly reduce the remaining stress (internal stress) in the work piece while basically retaining the original strength and hardness of the material. For beryllium bronze, such treatment under 150°-200° C and retaining the temperature for not over 2 hours can eliminate (or more correctly, partially eliminate) the remaining stress produced by cutting, straightening and cold forming, thus stabilizing the precision of the shape and the dimensions of precision parts during the course of long term use. But it should be pointed out that because the aging temperature is higher than the temperature for annealing to remove stress, the ability of aging to remove the remaining stress is greater than annealing to remove stress, so if the work piece needs to undergo aging after cutting, straightening and cold forming, it will not require annealing to remove stress.

Table 7. Effects of Quenching and Annealing Below the Critical Point Upon the Mechanical Properties of a Band (Thickness 5 mm) of QBe 2 (1.97% Be, 0.46% Ni) Deformed 50% by Cold Rolling (10)

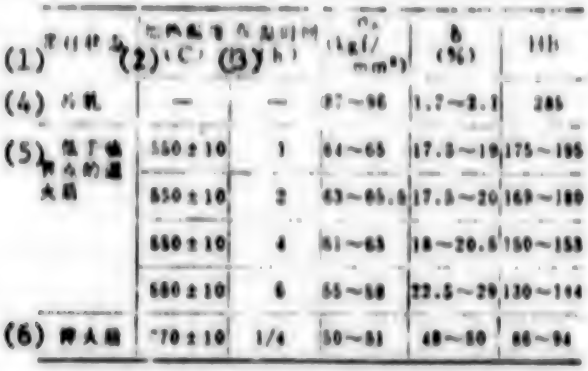

(1)	(2) (°C)	(3) (h)	σ_b (kgf/mm²)	δ (%)	HB
(4)	—	—	87~96	1.7~2.1	205
(5)	550 ± 10	1	64~65	17.5~19	175~195
	550 ± 10	2	63~65.5	17.5~20	169~180
	550 ± 10	4	61~63	18~20.5	150~153
	580 ± 10	6	55~58	22.5~29	130~144
(6)	770 ± 10	1/4	50~51	48~50	86~94

Key:

1. State of band material
2. Heating temperature
3. Time of temperature retention
4. Cold rolling
5. After annealing below critical point
6. After quenching

3. Heat Treatment in the Fixture

To obtain the correct shape and precise dimensions of the work pieces of beryllium bronze after heat treatment, it is necessary to affix the work pieces in appropriate fixtures for aging. When carrying out heat treatment in fixtures, the design of the fixtures must follow the following principles:

A. The fixture must have minimum weight;

B. Overly tight pressure must be avoided so that the tightening screws and threads will not fall off and the fixture will not bend or deform;

C. Clamps should only hold key positions of the work piece;

D. The least number of tightening screws should be used to hold the maximum number of work pieces;

E. Bending of the fixture should be reduced to a minimum to increase its useful life;

F. When the shape of the work pieces allows, the fixture should be designed so that the work pieces can be placed on top of each other (Diagram 5).

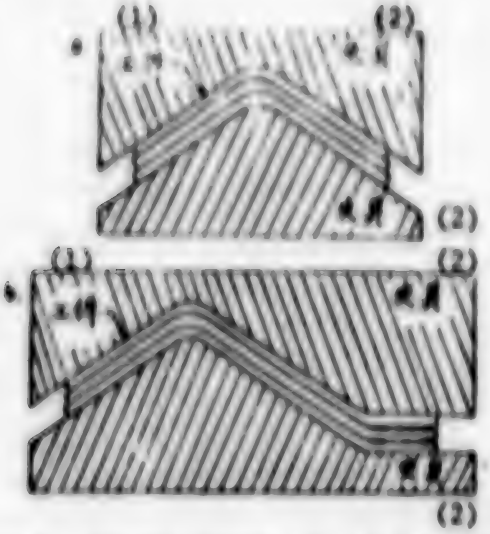

Diagram 5. To obtain a strict common error in the dimension of work pieces, the diagram illustrates work pieces which can be placed on top of each other (a) and work pieces which cannot be placed on top of each other (b) during aging in a fixture (9)

Key:

1. Work piece
2. Fixture

If the following rules are kept in mind, precise control of the shape of work pieces of beryllium bronze heat treated can be realized.

A. During precipitation-hardening or aging, as the strengthening phase separates out, beryllium bronze will undergo about 0.2% of linear contraction.

B. According to the principle of Le Chatelier, the area of elasticity or remnant stress will quickly undergo precipitation-hardening. Therefore, the area of the work piece acted upon by pressure and stress will first contract in the pressured direction, causing permanent deformation in this direction.

C. The elastic stress (ordinarily originating from the holding forces of the fixture) applied on the work piece in heat treatment produces a more intense effect than the remaining stress after plastic deformation in aging dynamics.

D. Work pieces quenched after they had already been formed and actually without stress will not visibly warp and deform if they are not subjected to stress during the course of precipitation-hardening.

E. Aging is additive. For example, if a peak value hardness can be obtained by aging for 2 hours under 330° C, the same result can also be obtained by aging twice under 330° C for 1 hour each time (after each aging process, the piece is quickly cooled to room temperature).

F. Uneven metallurgical structure will cause uneven precipitation and hardening. Dual crystalline grain structure (mixture of large and small crystal grains), uneven temperature for solid solution treatment or quenching and cooling, and variation in the beryllium content (partial separation) are all examples of unevenness.

G. To obtain the best compliance, work pieces should be slightly over aged. Over aging can better eliminate stress and thus stabilize the shape fixed by the fixture. The most frequently used method is short-time high-temperature aging (for example, aging for 15 to 45 minutes under 370° C). This produces the best ability in the parts to resist wander and resist relaxation when in use. But to obtain these benefits means some sacrifice of strength and hardness.

H. There should not be any burr on the work pieces, or else the work pieces will not be able to fit the fixture precisely.

The following are some examples of heat treatment in fixtures to obtain the required shapes and precise dimensions:

If a spiral spring of beryllium bronze wire or band formed by precipitation and hardening is aged in a free state (at 343° C for 2 hours), it will first contract because of the existence of remnant pressure stress caused by cold forming on the inside surface of the spiral, causing a permanent deformation and making the spring curl more tightly and the dimensions become smaller. To avoid such change, the spring must first be quenched in a fixture (water quenched from 790° C) so that the work piece is in a relatively stress-free state, then it is aged in a free state (at 343° C for 2 hours) and it will almost not deform or if it does, the deformation will be very minute. (11)

Diagram 6 (a) shows a U-shaped and a ring-shaped beryllium bronze spring that have just been formed; after aging, the shapes shown in Diagram 6 (d) are required. The recommended aging technique is: 1) First partially age the work piece already formed in a free state under 330° C for 1 hour. Because of the remnant pressure stress on the inner surface of the circular arc produced at the time of bending, the piece will first contract during this stage of aging, causing the spring opening to close slightly as illustrated in Diagram 6 (b). 2) The spring that has been partially aged is then cooled to room temperature, then it is installed on a steel rod or a mandrel (fixture) that has been precisely machine processed so that the outer surface of the circular arc is subjected to elastic pressure stress. [no point 3 is given] 4) The spring installed on the steel rod or the mandrel is then aged under 330° C for 1 hour. Then the outer surface of the circular arc of the spring will contract first, and at the same time the spring will form the shape fitting the fixture, and thus the desired shape is obtained.

Logically speaking, forming the two types of springs described above in the shapes shown in Diagram 6 (b) and then directly installing them on a steel rod or mandrel and aging them continuously for 2 hours should produce the same results and the technical procedures should be greatly simplified, but actual experiments did not produce satisfactory results. Because it was difficult to estimate the appropriate amount of overdeformation, the gap of the mouth of the springs subjected to this simplified aging process was often too small or too large. Therefore, for springs with openings similar to those shown in Diagram 6, the two-step aging process described above is a basic measure in the use of simple fixtures to obtain control over the shape of work pieces.

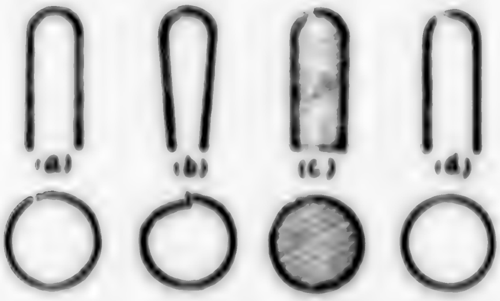

Diagram 6. Order of Heat Treatment of the U-Shaped Spring (top) and the Ring-Shaped Spring (bottom) (11)

(a) After forming (b) Opening closes slightly after aging for 1 hour under 330° C in free state (c) Installed on the steel rod or mandrel (fixture) and aged for the final time for 1 hour under 330° C (d) Work piece with the desired shape after completion

For beryllium bronze work pieces of more complex shape, such as the diaphragm shown in Diagram 7, the center and the edges of the work piece must all be held in a fixed position during heat treatment. For the wave-shaped diaphragm ring, only the top and bottom parts need to be in contact with the fixture so that they will be appropriately held down.

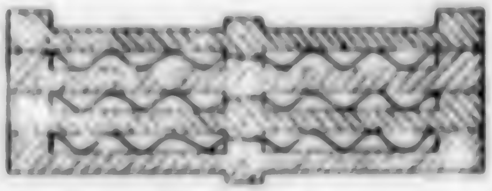

Diagram 7. Fixture That Can Be Piled Up for Use in Heat Treatment of Diaphragms (12)

V. Acid Washing of Beryllium Bronze

When beryllium bronze is heat treated in a nonprotective furnace gas, an oxidized film of the form BeO will form on the surface. According to the requirements of external appearance or of later tin welding, silver welding, electroplating, pressure processing or other operations, this oxidized film can easily be removed by acid washing.

The procedures to remove the oxidized film on the surface of beryllium bronze work pieces by acid washing are as follows:

1) The work piece is submerged in a water solution of sulfuric acid (specific gravity of 1.83) of a concentration of 20% to 30% (percentage by volume) of 70° to 80° C until the black oxidized film disappears;

2) The work piece is thoroughly washed in cold water;

3) The work piece is submerged in a water solution of nitric acid (specific gravity of 1.4) of a concentration of 30% (percentage by volume) for shining to remove the remnant black oxidized film (CuO) and any possibly remaining red spots (Cu_2O); the time of soaking can be determined by experiment but it should not be too long to avoid corrosion of the basic metal;

4) The work piece is thoroughly washed in cold water;

5) The work piece is soaked in soap solution to neutralize the acid and to remove remnant acidic solution;

6) The work piece is washed in hot water;

7) The work piece is dried by blowing it with compressed air or by other methods.

To obtain good results in acid washing, oil and other lubricants on the surface of the work piece must be removed. If the work piece must be quenched or aged before acid washing, the work piece must first be carefully degreased before heating, and at the same time, between heat treatment and washing, care should be taken so that the work piece is not dirtied by oil. In addition, the acid washing trough should not contain any steel or iron scrap or other objects dropped into it, or else red spots will appear on the work piece because of precipitating copper.

FOOTNOTES

1. Metals Handbook, 8th Edition, Vol 8, ASM, 1973, 271.

2. Heavy Nonferrous Metal Materials Processing Handbook (First Volume), Metallurgical Industry Press, 1979, 208.

3. 1976 Annual Book of ASTM Standards, Part 6, Copper and Copper Alloys, B194-74.

4. Guide to Metals, Vol 2, "Machine Building," 1976, 437-439.

5. Togamiyama Seikau: Nonferrous Metal Materials (Standard Metallurgy Lecture 4), Corona Company, 1963, 103.

6. Metals Handbook, 8th Edition, Vol 1, ASM, 1961, 1037.

7. Metals Handbook, 8th Edition, Vol 2, ASM, 1964, 288.

8. K.G. Wikle: Heat Treatment of Beryllium Copper Alloys, Part V, "Industrial Heating," 11, 1973, 24.

9. Metals Handbook, 8th Edition, Vol 2, ASM, 1964, 289.

10. S.I. Berman: Copper Alloys, Their Properties, Applications and Processed Materials, publisher of "Metallurgy," Moscow, 1966, 120.

11. K.G. Wikle and L.D. Alspach: Beryllium Copper Alloys, "Machine Design," 36, 1964, 17, 154.

12. K.G. Wikle: Heat Treatment of Beryllium Copper Alloys, Part IV, "Industrial Heating," 1973, 12, 41.

9296
CSO: 4008/334

TABLE OF CONTENTS OF 'JISUANJI XUEBAO' NOS 1-3, 1981

Beijing JISUANJI XUEBAO [CHINESE JOURNAL OF COMPUTERS] in Chinese Vol 4 Nos 1-3, 1981

[Vol 4 No 1, 1981 inside back cover]

[Text] On the Design of the System Programming Language XCY......Xu Jiafu [1776 1367 4395], Nanjing University; Zhong Cuihao [0112 5488 6275], Institute of Computing Technology, Chinese Academy of Sciences; Yang Fuqing [2799 5346 3237], Beijing University (10)

The Generalized Precedence Grammar......Lu Buqian [7120 3067 6870], Institute of Mathematics, Chinese Academy of Sciences (20)

The GP-Grammar and the Matching Precedence Parsing Algorithm ......Hao Kegang [6787 0344 0474], Xibei University (27)

Some Mathematical Problems of the Design and Management of a Kind of Data Processor (II)......Dong Zeqing [5516 3419 3237], Institute of Applied Mathematics, Chinese Academy of Sciences; Chen Zhonglian [7115 1813 6647], Institute of Systems Science, Chinese Academy of Sciences (38)

The Features of the 151-3/4 Large Computer System......Ci Yungui [1964 0061 2710], Changsha Institute of Technology (47)

A Fast Algorithm for Finding Boolean Differences...... Liu Chunhe [0491 2504 0735], Harbin Institute of Technology (55)

A Fast Planarity Algorithm......Ye Daxing [5509 1129 5281], Institute of Computing Technology, Chinese Academy of Sciences (68)

Research Notes

Random Nonrelativity of Random Hash......Lu Weiming [7120 4850 2494], Institute of Mathematics, Chinese Academy of Sciences (75)

Efficiency of Parallel Memory......Fang Xinwo [2455 0207 2053], Institute of Computing Technology, Chinese Academy of Sciences (80)

Introducing the Chinese Computer Society...... (82)

[Vol 4 No 2, 1981 inside back cover]

[Text] Special Reports on Computerized Chinese Character Editing and Laser Typesetting System

A Brief Introduction to the Computerized Chinese Character Editing and Laser Typesetting System......Wang Xuan [3769 6693], Beijing University (89)

Laser Phototypesetter of Chinese Characters......Zhang Heyi [1728 0678 5030] and Li Xinzhang [2621 2450 4545], both of Beijing University; et al. (95)

Problem-oriented CL Language and Its Implementation...... Chen Kunqiu [7115 1024 9460], Ding Aili [0002 7224 7787] and Bai Minzhu [4101 2404 3796], all of Beijing University; Dong Xiafen [5516 7209 5358], Shandong Electronics Research Institute; et al. (102)

The Design and Implementation of the Operating System CL ......Yu Shiwen [0205 1102 3080] and Chen Kunqiu [7115 1024 9460], both of Beijing University; Fu Guotai [0265 0948 3141], Weifang Computer Factory, Shandong Province (110)

Computer-aided Design of Newspaper Layout......Wang Zengkang [3769 1073 2123] and Sun Chengxuan [1327 2110 5503], both of the Technical Research Center, Xinhua News Agency; Yang Kongquan [2799 1313 3123], Beijing University (115)

Hierarchical Storage (Hierarchy) for High Quality Chinese Fonts and Its Transfer Control......Chen Baojue [7115 5508 3778], Dong Shihai [5516 1102 3189], Wu Shiqi [0702 0013 3825] and Lu Zhimin [0712 0037 2404], all of Beijing University; Xiang Yang [0686 7122], Xu Xinghai [1776 5281 3189] and Zhang Deyuan [1728 1795 3104], all of Weifang Computer Factory, Shandong Province (123)

Microprogrammed Firmware for Chinese Character Generation ......Wang Xuan [3769 6693] and Chen Baohua [7115 0202 5478], both of Beijing University; Li Erxi [2621 1422 3305], Yan Kaifu [0917 7030 1381] and Tang Yuhai [3282 3768 3189], all of the Weifang Computer Factory; You Jilin [1429 4949 2651], Guo Lujiang [6753 4845 3068] and Jin Fangxia [6855 2499 7209], all of the Technical Research Center, Xinhua News Agency (129)

Scanning Control Method for Laser Typesetter and the Formation of Page Layout......Pei Kunshou [5952 0981 1108] and Shao Bingzhang [6730 4426 4545], both of Beijing University; Hang Lingyun [2635 0407 0061], Weifang Computer Factory (136)

A Chinese Terminal System with a Shared Font Store......Gan Shengyu [3927 5110 0056], Northwest Institute of Telecommunication Engineering; Pei Kunshou [5592 0981 1108], Beijing University; Xiao Ruijie [5135 3843 7132], Wuxi Computer Factory (145)

Laser Phototypesetter with Four Electro-optical Modulators......Li Xinzhang [2621 2450 4545], Zhang Heyi [1728 0678 5030] and Zhao Hong [6392 7703], all of Beijing University; Liu Decai [0491 1795 2088], Hangzhou 522 Factory; Liu Guoguang [0491 0948 0342], Technical Research Center, Xinhua News Agency (150)

Overcoming the Hindrances in High-speed Pipeline Computers by means of a Combination of Hardware and Software--Conditional Operation and the Treatment of Sequential Subscript List......Gao Qingshi [7559 1987 3740], Zhang Xiang [1728 4382] and Wang Jiamo [3769 0857 6206], all of the Institute of Computing Technology, Chinese Academy of Sciences (156)

[Vol 4 No 3, 1981 on back cover]

[Text] The Verification of Monitors and the Incompleteness of Hoare Axiomatic Systems......Zhou Chaochen [0719 1560 1057], Institute of Computing Technology, Chinese Academy of Sciences (173)

The Vectorization of FORTRAN Do-loops......Wu Mingxia [0702 2494 7209] and Chen Huowang [7115 3499 2489], both of the Changsha Institute of Technology (180)

The Design of a Vector FORTRAN Language and Its Compiler......Zhang Zhaoqing [1728 0340 1987], Cheng Hu [4453 5706] and Chen Shuqing [7115 2885 3237], all of the Institute of Computing Technology, Chinese Academy of Sciences; Liu Yuanming [0491 1401 0682], Beijing Ninth Institute (187)

Address Calculation and Loop Optimization in a Vector FORTRAN Compiler......Jia Deping [6328 1795 1627] and Zhang Zhaoqing [1728 0340 1987], both of the Institute of Computing Technology, Chinese Academy of Sciences (196)

Nonuniformity and Nondeterminacy of Parallel Processing on One Kind of SIMD Computer......Chen Shuqing [7115 2885 3237] and Wei Jun [7614 6511], both of the Institute of Computing Technology, Chinese Academy of Sciences (204)

Expression Optimization for Pipeline Computers......Zhao Jihua [6392 3444 5478], Chen Shuqing [7115 2885 3237] and Zhang Zhaoqing [1728 0340 1987], all of the Institute of Computing Technology, Chinese Academy of Sciences; Liu Kuanming [0491 1401 0682], Beijing Ninth Institute (210)

A New Logical Design Methodology--The Direct Implementation of Predicate Calculus t Formulas on Synchronous Sequential Circuits......Jiang Mingde [3068 2494 1795], Chengdu Institute of Telecommunication Engineering (221)

A Rapid Method for Finding Special Solutions of Boolean Equations......Wang Wenzhang [3769 2429 4545], Xiangtan University (229)

A Fast Computer Algorithm for Rotation Large Matrices by 90°......Wang Xinmin [3769 2450 3046], Space Science and Technology Center, Chinese Academy of Sciences (234)

Research Notes

An Investigation of the Optimal Inhibiting Current in Coincident-Current Core Memories......Xu Xiulan [1776 4423 5695], Beijing Posts and Telecommunications Institute (238)

9717
CSO: 4008/362

TABLE OF CONTENTS OF 'FUDAN XUEBAO (ZIRAN KEXUE BAN)' NO 1, 1981

Shanghai FUDAN XUEBAO (ZIRAN KEXUE BAN) [FUDAN JOURNAL (NATURAL SCIENCES)] in Chinese Vol 20 No 1, 1981 preceding p 1

[Text] An Improvement on Hayman Regularity Theorems and Fitzgerald Inequalities......Ren Fuyao [0117 4395 1031] (1)

On the Error Bounds of Splines......Chen Tianping [7115 1131 1627] (15)

Some Theorems on Complex Space Form......Huang Chengchao [7806 1004 6389] (23)

On a Generalization of Minlos Theorem......Yang Yali [2799 0068 4539] (31)

Reductive Algebras and GCR Algebras......Xia Jingbo [1115 4842 0590] (38)

Real Decomposable Operators......Tong Yusun [4547 5940 1327] (51)

Quasi-positive Definite Functional and Symmetric Representation......Zhang Yinnan [1728 5593 0589] (61)

Phase Transitions in Chiral Symmetric σ Model......Ni Guangjiong [0242 0342 3518] and Su Rukeng [5685 3067 6972] (67)

Calibration of Quarter Wave Plates......Xu Keshou [1776 0344 3769/1108] and Zhang Zhiming [4545 1807 7686] (77)

The Observation of a Nonlinear Effect in Spinach Chloroplasts......Liu Yixian [0491 0001 0341], Zhao Yansheng [6392 5888 6141] and Li Funing [2621 1381 6900], et al. (82)

On the Central Limit Theorem for the Sum of Random Numbers of Independent Random Variables......Ouyang Guangzhong [2962 7122 0342 0022] (89)

Romberg Quadrature by Midpoint Rule and Fibonacci Sequence ......Qin Zengfu [4440 1073 1788] (94)

An Application of the Method of Approximation Theory on Invariant Subspaces......Cao Jiading [2580 1367 7844] (100)

The Boundary Value Problems for a Kind of Symmetric Positive Systems in Corner Regions......Shi Jiahong [2508 0857 7703] (105)

The Coefficient Estimates for the Inverse of Univalent Functions in the Unit Disk......Tan Delin [6223 1795 6775] and Chen Jixiu [7115 4764 0208] (109)

A Molecular Domain Model for the Isotropic-nematic Phase Transition......Zhu Yun [2612 5089] (114)

9717
CSO: 4008/372

TABLE OF CONTENTS OF 'XI'AN JIAOTONG DAXUE' NO 2, 1981

Xi'an XI'AN JIAOTONG DAXUE [JOURNAL OF XI'AN JIAOTONG UNIVERSITY] in Chinese Vol 15 No 2, Apr 81 preceding p 1

[Text] Xi'an Jiaotong University Since 1896...... (1)

Conditions of Sufficiency and Necessity for Global Asymptotic Stability of the Zero Solution of One-type of Aizeman's Problem for n = 2...... Li Xiwen [2621 1917 7186], Department of Mathematics (9)

Hydrogen Enhanced Crack Growth and Rate Controlling Processes in AISI 4340 Steel......Lu Yizhong [7120 3015 0022], Department of Engineering Mechanics (23)

A Study of Reheat Cracking in Welding Using the Implant Method......Zhang Xiangquan [1728 4161 2938], Chen Zexin [7115 3419 3512] and Zhou Guangqi [0719 0342 4388], et al., all of the Department of Mechanical Engineering (33)

An Investigation of Flow Characteristics of Air-Water Mixtures through Angle Pipes......Chen Xuejun [7115 1331 0193], Xi'an Jiaotong University; Zhu Caiguang [2612 2088 1639], Shanghai Power Generation Equipment Design and Research Institute (47)

The Minimum Fluidized Velocity of Fluidized Bed Boilers ......Zhang Yongzhao [1728 3057 3564], Wen Long [3306 7893] and Huang Xiangxin [7806 4382 2450], et al., all of the Department of Power Machinery Engineering (65)

Steady Flow Tests of the Swirling Inlet Ports of a Diesel Engine......Wang Ziyan [3769 1311 1693] and Jiang Deming [5592 1795 2494], both of the Department of Power Machinery Engineering (73)

An Approximate Method for Calculating the Electromagnetic Induction of Large Section Tubular Conductors and Its Application......Wu Lijian [0702 0536 1017], Department of Electrical Engineering (83)

The Theory of Treeing Inhibition Due to the Conduction Caused by Electric Field......Tu Demin [1458 1795 3046], Wu Lihuang [0702 0500 3552] and Wu Xuezheng [0124 1331 2973], et al., all of the Department of Electrical Engineering (95)

The Ellipsometric Study of Ion-implanted Layer (I)...... Chen Minqi [7115 2404 7784] and Luo Jinsheng [5012 2516 3932], both of the Department of Electrical Engineering (107)

Research and Discussion of Total Population Target in China ......Hu Baosheng [5170 0202 3932], Wang Huanchen [3769 3183 1057] and Zhu Chuzhu [2612 2806 3796], et al., all of the Institute of Systems Engineering (115)

Research on the Procedure of Experimentally Determining the Oil-film Stiffness and Damping Characteristics in Hydrodynamic Journal Bearings......Lin Jun [2651 6874], Qiu Damou [8002 1129 6180] and Liu Bingjun [0491 4426 6874], et al., all of the Department of Basic Courses (127)

Strength and Toughness of Medium-Carbon Steel Containing both Martensite and Ferrite......Song Yujiu [1345 0151 0046], Shen Lian [3088 5571] and Rao Qichang [7437 0796 2490], et al., all of the Research Institute of Strength of Metals (145)

Graduate Student Theses

A New Test Model of Synchronous Sequential Networks...... Ma Weiguo [7456 5898 0948], Department of Electrical Engineering (161)

Optimal Power Flow Solution......Shi Hanji [2457 3352 1015], Department of Electrical Engineering (163)

A Mintem-vector Method for Fault Diagnosis of Combinational Networks......Hou Yibing [0186 5030 2430], Department of Electrical Engineering (167)

9717
CSO: 4008/363

TABLE OF CONTENTS OF 'WULI' NO 3, 1981

Beijing WULI [PHYSICS] in Chinese Vol 10 No 3, 1981 on back cover

[Text] Knowledge and Progress

Models of Sodium Ionic Movement in MOS Systems......Xu Zhizhong [1776 5267 0022], Department of Physics, Fudan University (129)

Coder Aperture Imaging of 3-D Objects......Liu Liren [0491 4539 0086], Yin Yaozu [3009 5069 4371], Zhao Liying [6392 7787 5391], and Xu Chenliang [6079 5256 5328], all of the Shanghai Institute of Optics and Fine Mechanics, Chinese Academy of Sciences (134)

Progress in Intense Ion Beam Optics......Fang Jinqin [2455 6930 3237], Atomic Energy Research Institute, Chinese Academy of Sciences (140)

On the Nature of Physics and the Special Feature of Its Modern Development......Peng Huanwu [1756 2719 2976], Institute of Theoretical Physics, Chinese Academy of Sciences (147)

Research Reports

On the Stability of C32-type Transition Metal Borides...... Wang Wenkui [3769 2429 7608], Institute of Physics, Chinese Academy of Sciences (150)

Investigations of the Phenomenon of Weak-quenching of the Fluorescence in LNP Crystals......Wu Guangzhao [0702 0342 3564] and Zhang Xiurong [1728 4423 2837], both of the Shanghai Institute of Optics and Fine Mechanics, Chinese Academy of Sciences (152)

Measurements of the Compressibility of Liquids--The Compression Curves and Phase Transitions of Water and Carbon Tetrachloride......Wang Jifang [3769 4480 2455], Wang Ruju [3769 3067 5468] and He Shouan [0149 1108 1344], all of the Institute of Physics, Chinese Academy of Sciences (154)

X-ray Emission Spectrum and Distribution of the Ion Population Densities of Oxygen in a Laser-imploded Glass Microshell Target......Wu Cunkai [0702 1317 1956] and Lou Qihong [2869 4388 3163], both of the Shanghai Institute of Optics and Fine Mechanics, Chinese Academy of Sciences (157)

Free Oscillation Characteristics of Solid State Lasers Pumped by Electrodeless Discharges......Zhang Zunkui [1728 6690 6652] and Ye Maofu [5509 5399 4395], both of the Institute of Physics, Chinese Academy of Sciences (159)

Experimental Techniques

Development of a Large-area Plasma Source......Su Daren [4725 6671 0086], Li Wenlai [2621 2429 5490] and Liu Jiarui [0491 1367 3843], all of the Institute of Physics, Chinese Academy of Sciences (162)

Lectures

Geometrical Structure of Crystalline Surfaces......Shen Yuyi [3088 3022 3085], Department of Physics, Tianjin Teachers College (166)

History of Physics

On the Year of Discovery of the Universal Gravitation Law ......Yan Kangnian [7051 1660 1628], Natural History Research Institute, Chinese Academy of Sciences (172)

Translated Articles

Laue-Langevin Institute Expands......BMS (176)

Reference Material

Symbols, Units and Nomenclature in Physics...... (178)

China-United States Physics Examination and Application (CUSPEA) Examination Papers (II: Modern Physics)...... (191)

News and Information

Symposium on Statistical Physics and Condensed State Theory ......Tang Zhenhua (192)

Second National Symposium on Amorphous Materials and Physics Held in Kunming......Wang Zhenxi (inside back cover)

Short Communication of the First National Conference on Dielectric Physics......Wu Shuyao (inside back cover)

Luminescence Division of the Physical Society of China Established at the Second National Luminescence Conference Held in Xiamen......Lin Xiuhua (inside back cover)

9717
CSO: 4008/361

AUTHOR: LI Yonghong [2621 3057 3163]
TIAN Fengzuo [3944 7685 4373]
LI Zongquan [2621 1350 0356]
ZHANG Lide [1728 4539 1795]
LONG Qiyi [7893 6386 2496]
HE Yizhen [0149 1837 6297]

ORG: LI Yonghong and TIAN both of the Central Nonferrous Metals Research Institute, Ministry of Metallurgical Industry; LI Zongquan, ZHANG, LONG and HE all of the Institute of Metal Research, Chinese Academy of Sciences

TITLE: "*In Situ* Observation of Crack Nucleation and Propagation in -Titanium under Tensile Loading by HVEM"

SOURCE: Shenyang JINSHU XUEBAO [ACTA METALLURGICA SINICA] in Chinese Vol 17 No 2, Apr 81 pp 113-117

TEXT OF ENGLISH ABSTRACT: This paper presents the results obtained from the *in situ* observations of the crack nucleation and its propagation under tensile loading in HVEM. It was found that some slip bands appeared and slip steps formed at both ends of a slip band through the movement of a great deal of dislocations. The crack is initiated at the slip step due to the stress concentration. Once a crack has nucleated, it will propagate forward under the applied stress. The cracks propagate essentially in two ways: (1) during tensile loading, a large plastic thinning zone

[Continuation of JINSHU XUEBAO Vol 17 No 2, Apr 81 pp 113-117]

is formed near the crack tip. The crack propagates along the thinning zone in a discontinuous manner; (2) the main crack propagates by a mechanism of coalescence of microcracks in the vicinity of the crack tip. In addition, it was noticed that the grain boundary is not probably the preferential site of the crack nucleation and propagation in α-titanium.

AUTHOR: ZHAO Huitian [6392 1920 3944]
SHI Changxu [1597 2490 4872]

ORG: Both of the Institute of Metal Research, Chinese Academy of Sciences

TITLE: "Investigation of CoO Inoculant for Surface Grain Refinement of Cast Nickel-Base Superalloy Blades"

SOURCE: Shenyang JINSHU XUEBAO [ACTA METALLURGICA SINICA] in Chinese Vol 17 No 2, Apr 81 pp 118-123

TEXT OF ENGLISH ABSTRACT: The CoO inoculant composed of 20 percent CoO and 80 percent Al_2O_3 (fused alumina) is an effective nucleator to the cast nickel-base superalloy blades. After calcining CoO and Al_2O_3 powders under 1300°C for 2 hours, $CoO \cdot Al_2O_3$ spinel was formed on the surface of alumina particles. It has been detected by EMPA that metallic Co of fcc crystal structure deposits on the surface due to the fact that the $CoO \cdot Al_2O_3$ spinel is reduced by certain active elements contained in the cast nickel-base superalloys at elevated temperatures. This is checked with the relative stabilities of the oxides of Ti, Cr and Al contained in the alloy with CoO. This was also verified by the pure Ni blades for which there was no effect at all. Because of the similarity of the crystal structure and the lattice constants of the metallic Co and the superalloy, the Co particles can act as nucleators refining the grains. In production practice, if SiO_2 is precipitated in the local area of the inner surface of mold, covering the inoculant particles,

[Continuation of JINSHU XUEBAO Vol 17 No 2, Apr 81 pp 118-123]

the nucleation effect is markedly reduced. In order to prevent the metallic Co from remelting back, a lower pouring temperature is preferred. Therefore, to enhance the reduction of $CoO \cdot Al_2O_3$ a higher heating temperature of the mold is preferable.

AUTHOR: None

ORG: Phosphorus Segregation Research Group, Institute of Metal Research, Chinese Academy of Sciences

TITLE: "Observation of Phosphorus Segregation and Its Influence on Embrittlement in Steels"

SOURCE: Shenyang JINSHU XUEBAO [ACTA METALLURGICA SINICA] in Chinese Vol 17 No 2, Apr 81 pp 124-129

TEXT OF ENGLISH ABSTRACT: The phosphorus segregation in certain steels has been observed by means of metallography and EPMA. It was found that such a segregation may cause the intergranular fracture in steel which is confirmed by an Auger spectroscopic analysis. The coefficient of phosphorus segregation α seems to have a quantitative relationship with the deformation ratio θ of steels $\lg\alpha = A(1/\sqrt{\theta})$ where A is a material constant of working temperature and test condition. In addition, some influences of the local segregation of phosphorus upon the fracture toughness of steels were determined. The average J_{Ic} and K_{Ic} of normal specimens and ones with cracks through the segregation region and 9.87 and 7.68 kgf/mm, and 477 and 419 kgf/mm$^{3/2}$ respectively.

AUTHOR: ZHANG Qiyun [1728 0796 6663]
ZHENG Chaogui [6774 2600 6311]
HAN Wanshu [7281 8001 2579]

ORG: All of the Department of Chemistry, Beijing University

TITLE: "The Modification of Al-Si Eutectic Alloys with Rare-earth Elements"

SOURCE: Shenyang JINSHU XUEBAO [ACTA METALLURGICA SINICA] in Chinese Vol 17 No 2, Apr 81 pp 130-136

TEXT OF ENGLISH ABSTRACT: A systematic study has been made of the modification of Al-Si alloys with 11 individual rare-earth elements (La, Ce, Pr, Nd, Sm, Eu, Gd, Tb, Ho, Er and Y) and also mischmetal at a cooling rate of 70-80°C/min. The modifier was added into the alloys by the methods of both reciprocal reaction and electrolysis of corresponding binary molten salts of rare-earth chloride and KCl. From the metallographic observation, it was shown that Eu possesses the greatest modification ability, and La the next, and both of them are permanent modifiers. The modification ability of Ce, Pr, Nd and mischmetal is even weaker than that of La. It was also found that modification ability of rare-earth elements decreases rapidly with the decreasing of their atomic radii. The greatest modification ability of Eu may be referred to the leap of its atomic radius. Due to a similar reason, Yb (not investigated) would be expected to be another element possessing strong modification ability in lanthanide. Following lanthanide, from Sm to Ho the modification ability is negligible. Finally, under the conditions mentioned

[Continuation of JINSHU XUEBAO Vol 17 No 2, Apr 81 pp 130-136]

above, Er and Y did not show any modification effect on Al-Si eutectic alloy at all. According to the information that the atomic radius of Ac (2.03 Å) is somewhat greater than that of La (2.02 Å) and the modification ability may become greated in the order Y-La-Ac of the periodic table, it is deduced that the radioactive element Ac may have even greater modification ability than Eu. Thus the strongest modifiers would be elements La, Sr and Ac set on an oblique straight line in the periodic table. Therefore, it is assumed that the modification ability of a modifier may be the result of a certain combination of the valence electron charge number, the atomic number and the atomic radius of the modifier.

AUTHOR: LIU Wenxi [0491 2429 6007]
ZOU Meiyun [6760 5019 6663]
MA Fuben [7456 4395 2609]

ORG: None

TITLE: "The Morphology of Bainite in a 30CrMnSi Steel"

SOURCE: Shenyang JINSHU XUEBAO [ACTA METALLURGICA SINICA] in Chinese Vol 17 No 2, Apr 81 pp 137-147

TEXT OF ENGLISH ABSTRACT: The bainite transformation in a 30CrMnSi steel was studied by thin foil transmission electron microscopy. It was found that: (1) The lower bainite of twin rail mode or of side precipitation mode and the upper bainite of branch mode are present in the steel. The midribs occur in the lower bainite plates and the step-like fronts in the upper ones. (2) The determination of orientations not only between the cementite and bainite-ferrite matrix but also between the matrix and austenite has been carried out as:

$$(010)_\theta /\!/ (1\bar{1}\bar{1})_B,\ (1\bar{1}\bar{1})_B /\!/ (\underline{01}1)_A,$$
$$(103)_\theta /\!/ (101)_B,\ (101)_B /\!/ (\bar{1}\bar{1}1)_A$$

thus the bainite carbide precipitation from austenite may be proposed. (3) The formation of lower bainite seems to be analogous to the second stage of tempering, i.e., decomposition of retained austenite. During this stage, the correlation among four phases (austenite, ε-carbide, cementite and bainite ferrite) may

[Continuation of JINSHU XUEBAO Vol 17 No 2, Apr 81 pp 137-147]

possibly be expressed as a whole by the following parallelisms:

$$(\bar{1}\bar{1}1)_A \,//\, (000\bar{1})_\varepsilon \,//\, (103)_\theta \,//\, (101)_B,$$
$$(011)_A \,//\, (1\bar{2}10)_\varepsilon \,//\, (010)_\theta \,//\, (1\bar{1}\bar{1})_B,$$
$$(\bar{2}1\bar{1})_A \,//\, (\bar{1}010)_\varepsilon \,//\, (\bar{4}03)_\theta \,//\, (12\bar{1})_B$$

Specific close packed planes and directions are parallel in all these structures.

AUTHOR: LIU Zhengyi [0491 2973 5030]
HUANG Zhengzong [7806 2182 1350]
LIN Dingwen [2651 7844 2429]

ORG: LIU and HUANG both of the South China Institute of Technology; LIN of Huaqiao University

TITLE: "Morphology of Upper Bainite in a 55SiMnMo Steel"

SOURCE: Shenyang JINSHU XUEBAO [ACTA METALLURGICA SINICA] in Chinese Vol 17 No 2, Apr 81 pp 148-155

TEXT OF ENGLISH ABSTRACT: The morphology of upper bainite in a 55 SiMnMo steel under normalized conditions as well as its transformation in tempering has been observed by optical microscopy, TEM, SEM and X-ray diffraction. After austenitizing at 900°C for one-half hour and A.C., the upper bainite resulting was composed of ferrite and 30-35 percent carbon enriched austenite platelet, however, no carbide appeared until tempering treatment. The tempering temperature for carbide precipitation was found to be 400°C, and the tempering products, the so-called "tempered bainite," consisted of ferrite, carbide and 3-5 percent austenite. The rate of crack propagation da/dN of the steel increases with the increase of tempering temperature and reaches its maximum at about 400°C, acccompanied by a relevant change of fracture type from the quasi-cleavage to the cleavage.

AUTHOR: XU Wenchong [1776 3306 1504]
WANG Junjian [3769 0193 0256]
SU Xiujin [5685 4836 6930]
LI Zhihua [2621 1807 5478]

ORG: All of the Central Iron and Steel Research Institute, Ministry of Metallurgical Industry

TITLE: "Effect of the Modulated Structure on Physical Parameters of a NiFeNbAl Alloy"

SOURCE: Shenyang JINSHU XUEBAO [ACTA METALLURGICA SINICA] in Chinese Vol 17 No 2, Apr 81 pp 156-160

TEXT OF ENGLISH ABSTRACT: The alteration of the microstructure of a NiFeNbAl alloy has been observed under various heat treatments. It was shown that the magnetic properties and other physical parameters are immediately dependent on its microstructure. The alloy of 79 percent Ni-Fe-8 percent Nb-1.2 percent Al already has produced such properties as: μ_0 = 15-20 kGs/Oe, μ_m = 100-150 kGs/Oe, H_c = 0.015-0.03 Oe, B_s = 5200 Gs, ρ = 82-85 $\mu\Omega$/cm, HV = 290, after being treated by heating to 1150°C for 2 hours and 970°C aging 2 hours. An application of the alloy to the magnetic recording may be available.

AUTHOR: LIU Shuzhen [0491 2885 2182]

ORG: Research Institute of Wuhan Iron and Steel Company

TITLE: "Vacuum Vaporization of Certain Elements in Carbon-saturated Iron Melt"

SOURCE: Shenyang JINSHU XUEBAO [ACTA METALLURGICA SINICA] in Chinese Vol 17 No 2, Apr 81 pp 161-167

TEXT OF ENGLISH ABSTRACT: The behavior of vaporization of S, Mn, Cu, Si and P in carbon-saturated iron melt has been investigated with respect to the effects of smelting time and temperature, as well as pressure in the vacuum chamber and specific surface area of melt in a vacuum induction furnace. It was shown that an arrangement in vaporizability of these elements may be properly made, and a maximum rate of vaporization for S, Mn and Cu occurs at 1330°C.

AUTHOR: WANG Zhichang [3769 0037 2490]

ORG: Shanghai Institute of Nuclear Research, Chinese Academy of Sciences

TITLE: "Thermodynamics of Multicomponent Systems with Constant Partial Molar Quantity $\bar{\Psi}_0$--Thermodynamical Aspect of Iso-$\bar{\Psi}_0$ Rule of Zdanovskii or Turkdogan Type"

SOURCE: Shenyang JINSHU XUEBAO [ACTA METALLURGICA SINICA] in Chinese Vol 17 No 2, Apr 81 pp 168-176

TEXT OF ENGLISH ABSTRACT: A thermodynamical equation of n-component ($n \geq 3$) systems with constant partial molar quantity $\bar{\Psi}_0$ was derived for the interval between $\bar{\Psi}_0^0$ and $\bar{\Psi}_0$, i.e.,

$$(\Delta\bar{\Psi}_k)_{0,\bar{\Psi}_0} - (\Delta\bar{\Psi}_k)_{0,\bar{\Psi}_0^\circ} = \int_{\bar{\Psi}_0^\circ}^{\bar{\Psi}_0} \lambda_k d\bar{\Psi}_0$$

where $(\Delta\bar{\Psi}_k)_{0,\bar{\Psi}_0} = [(\bar{\Psi}_k)_0 - \bar{\Psi}_{k(0)}]_{\bar{\Psi}_0}, \; (\Delta\bar{\Psi}_k)_{0,\bar{\Psi}_0^\circ} = (\Delta\bar{\Psi}_k^\circ)_{0,\bar{\Psi}_0^\circ}$

and $\lambda_k = \left\{\frac{1}{x_{k(0)}} - \left[\frac{\partial(1/x_i)}{\partial(x_k/x_i)}\right]_{x_k}\right\}_{\bar{\Psi}_0}$

For such systems that obey the Zdanovskii-type rule, $\left(\sum_k \frac{x_k}{x_{k(0)}}\right)_{\bar{\Psi}_0} = 1 \; [1 \leq k \leq (n-1)]$,

one of the simple solutions of the equation may be:

$$(\Delta\bar{\Psi}_k)_{0,\bar{\Psi}_0} - (\Delta\bar{\Psi}_k^\circ)_{0,\bar{\Psi}_0^\circ} = 0$$

[Continuation of JINSHU XUEBAO Vol 17 No 2, Apr 81 pp 168-176]

For certain systems that obey the Turkdogan-type rule, $\left(\frac{x_1}{x_{1(0)}} + \sum_j \frac{x_j}{K_j x_{j(0)}}\right)_{\bar{\Psi}_0} = 1$,

the solution may be:

$$(\Delta\bar{\Psi}_1)_{0,\bar{\Psi}_0} - (\Delta\bar{\Psi}_1^\circ)_{0,\bar{\Psi}_0^\circ} = 0$$
$$(\Delta\bar{\Psi}_j)_{0,\bar{\Psi}_0} - (\Delta\bar{\Psi}_j^\circ)_{0,\bar{\Psi}_0^\circ} = {}_{\Psi}K_j \qquad [2 \leq j \leq (n-1)]$$

For example, if Ψ represents volume, heat capacity or enthalpy: $\Delta\Psi = 0$ when (n-1) binary systems of the same $\bar{\Psi}_0$ value are mixed up to compose an n-component system obeying the Zdanovskii-type iso-$\bar{\Psi}_0$ rule; and $\Delta\Psi = \sum_j K_{\Psi j} Y_j$ when (n-1) binary systems of the 0 component are mixed up to compose an n-component system obeying the Turkdogan-type iso-$\bar{\Psi}_0$ rule.

If Ψ represents Gibbs free energy: the activities of the k component in an n-component system obeying the Zdanovskii-type iso-μ_0 rule may be written as a Raoult-type equation: $a_k/a_{k(0)} = X_k$; and the activities of component 1 and each component j in the n-component system obeying the Turkdogan-type iso-μ_0 rule may be written as Raoult- and Henry-type equations, $a_1/a_{1(0)} = X_1$ and $a_j = K_j^\circ X_j$ respectively.

Satisfactory verifications of the aforementioned results have been made for aqueous solutions, liquid alloys or molten salts.

AUTHOR: BATU [1572 0956]
LEI Qiongzhi [7191 8825 5347]

ORG: Both of the Institute of Metal Research, Chinese Academy of Sciences

TITLE: "Dynamical Behavior of a Dislocation Group Containing a Source. I. Computer Simulation of the Glide Motion of a Dislocation Group Emitted from a Source"

SOURCE: Shenyang JINSHU XUEBAO [ACTA METALLURGICA SINICA] in Chinese Vol 17 No 2, Apr 81 pp 177-184

TEXT OF ENGLISH ABSTRACT: According to $\nu = c_0(\tau/\tau_0)^m$ and the condition of dislocation source operation, the glide motion of a dislocation group emitted from a source under a constant applied stress is simulated on a computer by using experimental data of isolated dislocation velocity in silicon crystals. The following conclusion is obtained:

1. The velocity of a leading dislocation in a group emitted from a source is approximately 1.36 times the velocity of an isolated dislocation. This result agrees with the experimental ones obtained in silicon crystals.
2. The average velocity of all dislocations in a group emitted from a source is equal to the velocity of an isolated dislocation.
3. In a dislocation group emitted from a source, the average density of all dislocations is proportional to τ_a, and the rate of generation of dislocations from a source is found to be:

$$\frac{dN}{dt} \propto \tau_a^{m+1} e^{-Q/kT}.$$

AUTHOR: WANG Guijin [3769 2710 6855]
KANG Zhenchuan [1660 2182 1557]
ZHAO Bolin [6392 0130 7792]

ORG: WANG of the Central Iron and Steel Research Institute, Ministry of Metallurgical Industry; KANG of the Beijing Institute of Metallurgy Research; ZHAO of the Beijing Institute of Iron and Steel Technology

TITLE: "On the Orientation Relationship between Transformation Product and Parent Phase"

SOURCE: Shenyang JINSHU XUEBAO [ACTA METALLURGICA SINICA] in Chinese Vol 17 No 2, Apr 81 pp 185-195

TEXT OF ENGLISH ABSTRACT: The cell volume $V^{(0)}$ of fcc/bcc and fcc/bct has been calculated for three orientation relationships. The orientation will be acceptable if its $V^{(0)}$ is larger than the others, and each one has its own range of lattice parameter ratio. Then the lower energy 0 lattice will appear when γ gets some particular value. It is suggested that the γ value can be changed locally by segregating or depleting solute atoms near the boundary so that the density of dislocation on the boundary can be decreased. The Zn segregation in α/β brass can be explained with this mode.

It is shown that the magnitude and direction of tetragonal distortion affect the $V^{(0)}$ considerably. A prediction of the reasonable distortion direction will be

[Continuation of JINSHU XUEBAO Vol 17 No 2, Apr 81 pp 185-195]

expected if the orientation and lattice parameter are given. But the fact that the orientation relationship between austenite and martensite in an Fe-C alloy changes from K-S to N-W can be explained satisfactorily if it is suggested that carbon atoms move to the transformation interface along the $\langle 11\bar{2}\rangle_f$ direction.

AUTHOR: YANG Chuanzheng [2799 0278 6927]
JIANG Xiaolong [1203 1420 7893]

ORG: Both of the Shanghai Institute of Metallurgy, Chinese Academy of Sciences

TITLE: "An X-ray Double Diffraction Line Method for Measuring Composition of Cubic Crystal System Solid Solution"

SOURCE: Shenyang JINSHU XUEBAO [ACTA METALLURGICA SINICA] in Chinese Vol 17 No 2, Apr 81 pp 196-205

TEXT OF ENGLISH ABSTRACT: The composition of a continuous or a limited solid solution obeying the Vegard theorem was successfully measured by two diffraction lines with single or double wavelength of X-ray. The relationship between the composition, x, and the diffraction angle difference, δ_x, for a cubic crystal system may be deduced as:

$$x \approx \frac{\delta_x - \delta_0}{\delta_1 - \delta_0}$$

where δ_0, δ_1 and δ_x are the differences between two diffraction angles for x = 0, 1 and x respectively. Certain typical examples were used to check the formula. In the case of deviation from the linear relation, a correct term, Δx, was introduced into it, and Δx vs x plot was found to satisfy a parabolical equation. Thus, the formula may be modified as:

$$x = \frac{\delta_x - \delta_0}{\delta_1 - \delta_0} + \Delta x_{max}\frac{4(\delta_x - \delta_0)(\delta_1 - \delta_x)}{(\delta_1 - \delta_0)^2}$$

[Continuation of JINSHU XUEBAO Vol 17 No 2, Apr 81 pp 196-205]

where Δx_{max} is the deviation at $x = 0.5$, eliminating the error induced from the linear approximation. Finally, the error of these two methods was discussed briefly. Because these methods depend only on the difference between diffraction angles, the error due to incorrect zero-position and specimen eccentricity can be eliminated. Therefore, the methods seem to be simple and rapid, and to have proper applicability as well.

AUTHOR: ZHANG Shutang [1728 2885 1016]
LIU Yurong [0491 3768 2837]

ORG: Both of the Central Iron and Steel Research Institute, Ministry of Metallurgical Industry

TITLE: "Differential Equation of Tension for Varying Strip Section and Mathematical Model for Dynamic Digital Simulation of Cold Tandem Rolling"

SOURCE: Shenyang JINSHU XUEBAO [ACTA METALLURGICA SINICA] in Chinese Vol 17 No 2, Apr 81 pp 206-212

TEXT OF ENGLISH ABSTRACT: The simplified Phillips' differential equation of tension, derived from Hooke's law on the assumption of uniform strip section, is conventionally used to date for the computation of cold tandem rolling. However, the strip operated through the stands in rolling practice is not uniform in section. An improved empirical differential equation of tension, especially for varying strip section, has been proposed as:

$$dt_{fi} = \frac{E}{h_i\left(\frac{l_1}{h_i} + \frac{l_2}{H_{i+1}}\right)}(v_{b(i+1)} - v_{fi})d\tau$$

under the consideration of the influence of step disturbance or dynamic gauge change. Based mainly on this equation, a mathematical model of dynamic digital

[Continuation of JINSHU XUEBAO Vol 17 No 2, Apr 81 pp 206-212]

simulation was made to trace the position of the stepped section. Certain examples of the simulation computation on a digital computer showed such marked errors as were still calculated by the equal section equation. However, a satisfactory representation of the dynamic process may result from the aforementioned equation.

AUTHOR: CHEN Liangshan [7115 0081 1472]

ORG: Institute of Metal Research, Chinese Academy of Sciences

TITLE: "Study of Loading Capacity of Miter Welding Joint"

SOURCE: Shenyang JINSHU XUEBAO [ACTA METALLURGICA SINICA] in Chinese Vol 17 No 2, Apr 81 pp 213-220

TEXT OF ENGLISH ABSTRACT: Based on the uniaxis tensile tests of several miter welding joints, a mathematical treatment for calculating loading capacity of the butt welding joints under complex stress conditions was worked out and an empirical formula is given as:

$$\sigma_{eq} = \sqrt{\sigma_w^2 + \sigma_w \tau_w^2}$$

The theoretical consideration of this formula is easily approached by the plasticity collapse and fracture mechanics. It is also clarified that the conventional understanding about the loading capacity in miter welding joints always being senior to that in perpendicular ones, and its related calculation as well, seems to be not entirely correct.

AUTHOR: CHEN Sen [7115 2773]

ORG: None

TITLE: "Stabilization and Super-stabilization of Austenite during Opposite Martensite Transformation in Certain Fe-Ni Base Alloys"

SOURCE: Shenyang JINSHU XUEBAO [ACTA METALLURGICA SINICA] in Chinese Vol 17 No 2, Apr 81 pp 221-224

TEXT OF ENGLISH ABSTRACT: The process of opposite martensite transformation in an Ni32Co4Cu alloy on heating has been studied. The stabilization and super-stabilization of austenite may be sufficiently displayed by the phase change cold work for austenite in the opposite transformation. After the double deep cold cyclic treatment, an alloy of lower linear expansion coefficient and stable microstructure under low temperature was obtained, which, in addition, was available to improve its mechanical properties and machinability.

AUTHOR: SHI Tiansheng [2457 1131 3932]
ZHANG Hong [1728 1347]
ZHENG Longru [6774 7893 1172]

ORG: All of Shanghai Institute of Metallurgy, Chinese Academy of Sciences

TITLE: "An Empirical Rule of Binary A-15 Phases Formation and Their T_c Variation"

SOURCE: Shenyang JINSHU XUEBAO [ACTA METALLURGICA SINICA] in Chinese Vol 17 No 2, Apr 81 pp 225-227

TEXT OF ENGLISH ABSTRACT: The binary A-15 phases formation and their T_c variation have been studied by means of the bond-parametric diagram. It was ascertained that the A-15 phases are located in a definite region on the plot of electron density e/a vs radii ratio of components r_A/r_B. The A-15 phase cannot form any longer for the ratio r_A/r_B over a certain critical value which varies with e/a periodically. On the plot, the T_c distribution of A-15 phases is shown with regularity. The A-15 phases with T_c higher than 1, 4.2, 10, 15 or 20 K are concentrated in the regions of corresponding isotherms. The ratio r_A/r_B, and e/a as well, may be important parameters in determining T_c. Compared with Matthias' rule, better results in determining the location of A-15 phases of high T_c have been obtained by consideration of both factors.

9717
CSO: 4009/255

AUTHOR: ZHU Ruizhao [2612 3843 0340]
XUE Heng [5641 2709]

ORG: Both of the Academy of Meteorology, Central Meteorological Services

TITLE: "The Wind Energy Resources in China"

SOURCE: Beijing TAIYANGNENG XUEBAO [ACTA ENERGIAE SOLARIS SINICA] in Chinese Vol 2 No 2, Apr 81 pp 117-124

TEXT OF ENGLISH ABSTRACT: In this paper, the hours and probabilities of effective wind velocity for power generation of 3, 4, 5, ..., 20 m/s were calculated respectively from 300 stations all over China. The densities of effective wind power and its percentages of time were further calculated.

Because of the complex topography in China, the influence of the Qinghai-Xizang (Tibet) Plateau on air density was also analyzed. In order to delineate its distributional features, maps of the density of effective wind power, its percentage of time, and the hours of ≥ 3 m/s and ≥ 6 m/s winds occurring were made.

AUTHOR: TANG Renyuan [0781 0117 6678]
GUO Zhongbao [6753 1813 0202]
LI Ge [2621 7245]

ORG: All of the Shenyang Institute of Mechanical and Electrical Engineering

TITLE: "Some Aspects of the Development and Design of a High-speed, High-efficiency Solar Energy Generator"

SOURCE: Beijing TAIYANGNENG XUEBAO [ACTA ENERGIAE SOLARIS SINICA] in Chinese Vol 2 No 2, Apr 81 pp 131-137

TEXT OF ENGLISH ABSTRACT: In order to increase the total efficiency of a small-scale solar energy power station, it is necessary to develop a special high-speed and high-efficiency solar energy generator. This paper has analyzed the various approaches to increasing the speed and efficiency of a generator by means of modern scientific and technical payoffs. Based on the analyses, a high-speed, high-efficiency solar energy generator has been developed. The most important distinction is that the generator is made of rare earth cobalt permanent magnets. The main characteristics of this generator are: rated output--3 kW, rated speed--20,000 rev/min, full load efficiency--91.5 percent, inherent voltage regulation--5.89 percent. Design considerations, rotor configuration with unique shrink ring and rotor fabrication of this type of generator are described in this paper. Recommendations are given for further machine improvements and material improvements.

AUTHOR: WANG Yifang [3769 5030 2455]
LI Zhilan [2621 5347 5695]

ORG: Both of the Department of Engineering Thermophysics, University of Science and Technology of China

TITLE: "A Comparison between the 'Once-through' and 'Thermosiphon' Solar Water Heaters and the Calculation of Their Thermal Efficiencies"

SOURCE: Beijing TAIYANGNENG XUEBAO [ACTA ENERGIAE SOLARIS SINICA] in Chinese Vol 2 No 2, Apr 81 pp 174-181

TEXT OF ENGLISH ABSTRACT: The "once-through" solar water heater has many advantages when compared with the "thermosiphon," which is being popularized in China gradually. The storage tank of the "once-through" can be placed lower than the collector, so it can be placed indoors and the heat loss will be reduced. On the other hand, the hot water can be obtained earlier than from the "thermosiphon." A preliminary calculation shows that the daily efficiency of the "once-through" is almost the same as that of the "thermosiphon." The authors believe that the "once-through" solar water heater can be adopted and popularized easier in China.

9717
CSO: 4009/273

END

END OF
FICHE
DATE FILMED

27 JULY 1981